Dual-Gated Photochromism for Both Directions of Azobenzene Isomerization via Metal Complexation

Koji Yamakawa ,[a] Masaki Yamamura*[b] and Tatsuya Nabeshima*[a,c]

[a] Graduate School of Science and Technology, University of Tsukuba, 1-1-1, Tennodai, Tsukuba, Ibaraki 305-8571, Japan.
[b] Center for Liberal Arts and Sciences, Faculty of Engineering, Toyama Prefectural University 5180 Kurokawa, Toyama, 939-0398, Japan.
[c] Department of Chemistry, Institute of Pure and Applied Sciences, Tsukuba Research Center for Energy Materials Science (TREMS), University of Tsukuba, 1-1-1, Tennodai, Tsukuba, Ibaraki 305-8571, Japan.
Tel&Fax: (+) 81-766-56-7500 E-mail: yamamura@pu-toyama.ac.jp

Table of contents

(1) **General methods**

All chemicals were reagent grade and used without further purification. All reactions were performed under a nitrogen atmosphere. Chromatography was performed using SiO_2-60N (0.063–0.212 mm; Kanto). A recycling preparative HPLC was performed using a JAI LC-908 equipped with JAIGEL-1H and -2H columns (GPC) using $CHCl_3$ as an eluent. Melting points were determined using a Yanaco and are uncorrected. The ^1H and ^{13}C NMR spectra were recorded by Bruker AVANCE400 (400 MHz) or AVANCE600 (600 MHz) spectrometer. Deuterated solvents were purchased from Cambridge Isotope Laboratories or Aldrich and used as received. In the NMR measurements, tetramethylsilane was used as the internal standard (0 ppm) for ^1H and ^{13}C NMR. MALDI-TOF mass spectra were recorded by an AB Sciex TOF/TOF5800. UV-vis absorption spectra were recorded by JASCO Ubest V-660. Photoirradiation was performed using a 400 W high-pressure mercury lamp of SEN Light Corporation through a colour filter.

(2) Synthetic procedure

Macrocyclic ligand *t*,*t*-**G** was synthesized as shown in Scheme S1. Compounds **4**[S1] and **2**[S2] were prepared according to literature procedure. Spacer ligands **L1**,[S3] **L2**,[S4] and **L3**[S5] were prepared according to literature procedure.

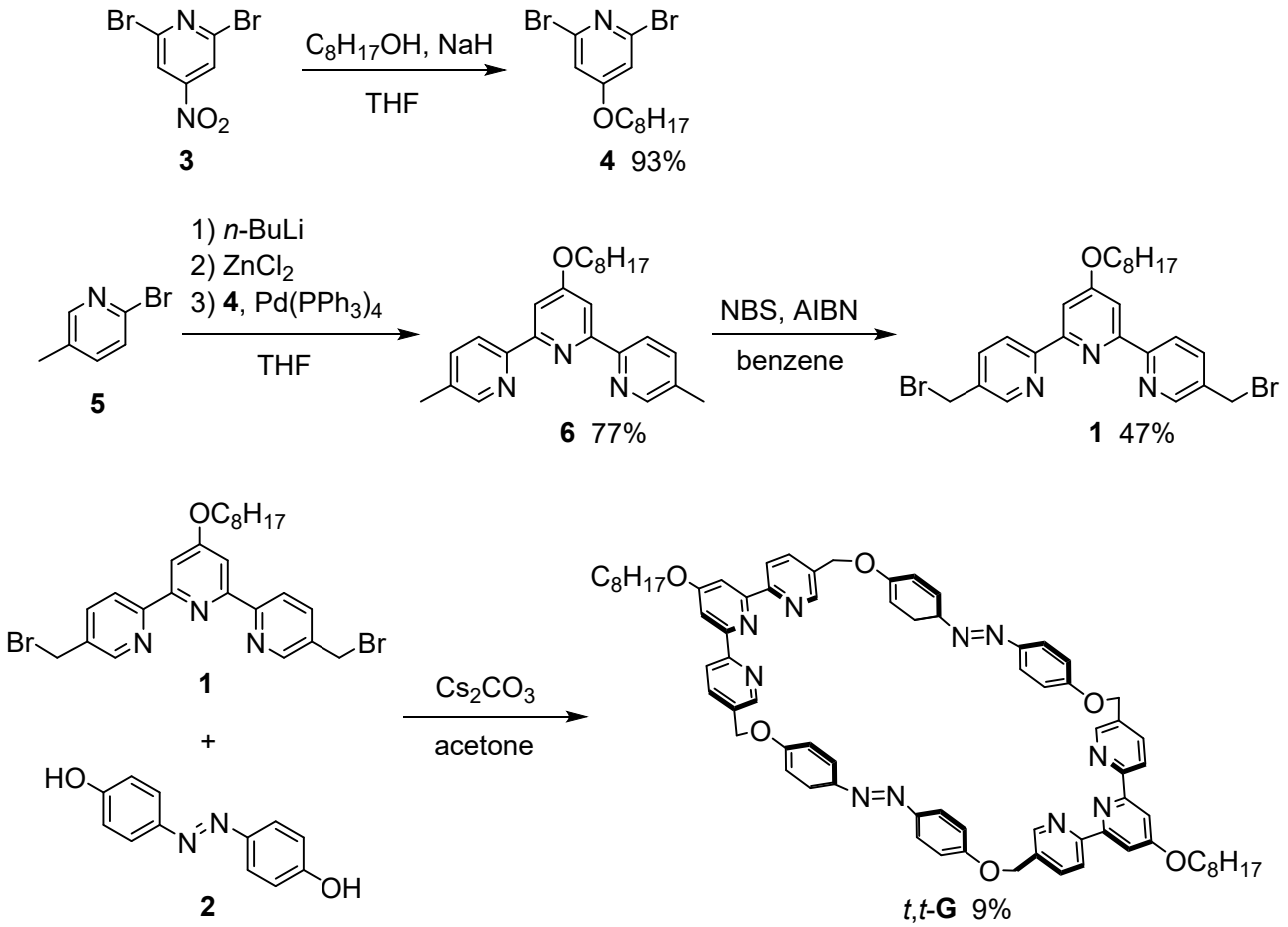

Scheme S1. Synthesis of *t*,*t*-**G**.

Synthesis of 6

To a THF solution (50 mL) of **5** (3.72 g, 21.6 mmol) was added BuLi/hexane (2.6 M, 9.0 mL, 23.9 mmol) at –78 ºC and then the mixture was stirred for 30 minutes. To the solution was added zinc chloride (3.94 g, 28.7 mmol) and then the mixture warmed to rt and stirred for 3 hours. To the solution was added a THF solution of **4** (3.94g, 10.8 mmol) and $Pd(PPh_3)_4$ (0.50 g, 0.43 mmol) and then the mixture was refluxed for 14 hours. To the mixture were added aqueous EDTA·Na_2 (10.7 g in 150 mL) and 1 M NaOH and an organic layer was separated. After extraction of an aqueous layer with chloroform, the combined organic layer was dried over $MgSO_4$ and evaporated. The crude products were separated by silica-gel column chromatography (eluent: chloroform/ethyl acetate (4/1)) to give colorless powder of **6** (3.25 g, 8.34 mmol, 77%).

6: colorless powder, mp > 300 °C; ^{1}H NMR (400 MHz, $CDCl_3$) δ 0.90 (t, *J* = 6.8 Hz, 3H), 1.23–1.40 (m, 8H), 1.49 (quin, *J* = 6.8 Hz, 2H), 1.84 (quin, *J* = 6.8 Hz, 2H), 4.21 (t, *J* = 6.8 Hz, 2H), 7.63 (d, *J* = 8.6 Hz, 2H), 7.94 (s, 2H), 8.49 (d, *J* = 8.6 Hz, 2H), 8.50 (s, 2H); ^{13}C NMR (100 MHz, $CDCl_3$) δ 14.1 (CH_3), 18.4 (CH_3), 22.7 (CH_2), 26.0 (CH_2), 29.1 (CH_2), 29.2 (CH_2), 29.3 (CH_2), 31.8 (CH_2), 68.2 (CH_2), 106.8 (CH), 120.9 (CH), 133.3 (C), 137.3 (CH), 149.4 (CH), 153.8 (C), 157.1 (C), 167.3 (C); MALDI-TOF–MS observed *m/z* 390.2530 ([**6**+H]$^+$) calcd for $C_{25}H_{32}N_3O$ 390.2545.

Synthesis of 1

A benzene suspension (30 mL) of **6** (299 mg, 0.768 mmol), NBS (289 mg, 0.742 mmol), AIBN (26 mg, 0.158 mmol) was refluxed for 9.5 hours. After evaporation, the residue was dissolved in chloroform and then washed with water. The organic layer was dried over $MgSO_4$ and evaporated. The crude products were separated by silica-gel column chromatography (eluent: chloroform/ethyl acetate (4/1)) to give colorless powder of **1** (198 mg, 0.362 mmol, 47%).

1: colorless powder, mp > 300 °C; ^{1}H NMR (400 MHz, $CDCl_3$) δ 0.89 (t, *J* = 6.8 Hz, 3H), 1.25-1.43 (m, 10H), 1.50 (quin, *J* = 6.8 Hz, 2H), 1.86 (quin, *J* = 6.8 Hz, 2H), 4.22 (t, *J* = 6.8 Hz, 2H), 4.56 (s, 4H), 7.87 (d, *J* = 8.2 Hz, 2H), 8.00 (s, 2H), 8.58 (d, *J* = 8.2 Hz, 2H), 8.68 (s, 2H); ^{13}C NMR (100 MHz, $CDCl_3$) δ 14.1 (CH_3), 22.7 (CH_2), 26.0 (CH_2), 29.0 (CH_2), 29.2 (CH_2), 29.3 (CH_2), 29.7 (CH_2), 31.8 (CH_2), 68.3 (CH_2), 107.8 (CH), 121.3 (CH), 133.7 (C), 137.4 (CH), 149.2 (CH), 156.1 (C), 156.5 (C), 167.4 (C); MALDI-TOF–MS observed *m/z* 546.0765 ([**1**+H]$^+$) calcd for $C_{25}H_{30}N_3O^{79}Br_2$ 546.0756.

Synthesis of *t*,*t*-G

An acetone solution (75 mL) of **1** (49.5 mg, 90.4 μmol), **2** (19.5 mg, 91.0 μmol), Cs_2CO_3 (119.5 mg, 0.367 mmol) was refluxed for 24 hours. After evaporation, the residue was dissolved in chloroform and then washed with water. The organic layer was dried over $MgSO_4$ and evaporated. The crude products were separated by alumina-gel column chromatography (eluent: chloroform) to give yellow powder of *t*,*t*-**G** (4.9 mg, 4.1 μmol, 9%). Quaternary carbon atoms in the terpyridine unit could be scarcely observed in ^{13}C NMR spectrum due to signal broadening and very low solubility of *t*,*t*-**G**.

t,*t*-**G**: yellow powder, mp > 300 °C; ^{1}H NMR (400 MHz, $CDCl_3$) δ 0.92 (t, *J* = 6.9 Hz, 6H), 1.26-1.43 (m, 16H), 1.47-1.57 (m, 4H), 1.86 (quin, *J* = 6.9 Hz, 4H), 4.21 (t, *J* = 6.9 Hz, 4H), 5.40 (s, 8H), 6.97 (d, *J* = 7.5 Hz, 8H), 7.76 (d, *J* = 7.5 Hz, 8H), 7.80 (d, *J* = 8.2 Hz, 4H), 7.99 (s, 4H), 8.53 (d, *J* = 8.2 Hz, 4H), 8.71 (s, 4H); ^{13}C NMR (100 MHz, $CDCl_3$) δ 14.1 (CH_3), 22.7 (CH_2), 25.9 (CH_2), 29.0 (CH_2), 29.2 (CH_2), 29.3 (CH_2), 29.7 (CH_2), 31.8 (CH_2), 67.3 (CH_2), 107.7 (CH), 115.7 (CH), 121.4 (CH), 124.4 (CH), 133.1 (CH), 147.3 (C), 147.5 (CH), 159.5 (C); Anal. Calcd for $C_{74}H_{74}N_{10}O_6$·1.3(H_2O): C, 72.68; H, 6.31; N,

11.45. Found C, 73.01; H, 6.38; N, 10.95; MALDI-TOF–MS observed *m/z* 1199.27 ([*t*,*t*-**G**+H]$^+$).

Synthesis of [*t*,*t*-1·Zn^{II}_2·L3](ClO$_4$)$_4$

To a chloroform solution of *t*,*t*-**G** (0.50 mM, 500 μL, 0.25 μmol) were added a methanol solution of $ZnClO_4 \cdot 6H_2O$ (2.0 mM, 250 μL, 0.50 μmol) and then a chloroform solution of **L3** (1.0 mM, 250 μL, 0.25 μmol). After evaporation of solvent, the crude yellow powder was dissolved in CD_3CN and the mixture was heated at 80 ºC for 21 hours. The NMR and ESI MS indicated the quantitative formation of [*t*,*t*-**G**·Zn^{II}_2·**L3**](ClO$_4$)$_4$.

[*t*,*t*-**G**·Zn^{II}_2·**L3**](ClO$_4$)$_4$: yellow powder; ^{1}H NMR (600 MHz, CD_3CN) δ 0.98 (t, *J* = 6.0 Hz, 6H), 1.39-1.24 (m, 4H), 1.47 (quin, *J* = 6.0 Hz, 4H), 1.54 (quin, *J* = 6.0 Hz, 4H), 1.67 (quin, *J* = 6.0 Hz, 4H), 1.86 (quin, *J* = 6.0 Hz, 4H), 2.08 (quin, *J* = 6.0 Hz, 4H), 4.60 (t, *J* = 6.0 Hz, 4H), 5.14 (s, 8H), 6.79 (d, *J* = 8.8 Hz, 8H), 7.65 (d, *J* = 8.8 Hz, 8H), 7.78 (dd, *J* = 6.7 Hz, 5.0 Hz, 4H), 7.93 (s, 4H), 8.08 (d, *J* = 5.0 Hz, 4H), 8.20 (d, *J* = 8.3 Hz, 4H), 8.25 (s, 4H), 8.43 (t, *J* = 6.7 Hz, 4H), 8.62 (d, *J* = 8.3 Hz, 4H), 9.25 (s, 4H), 9.26 (d, *J* = 6.7 Hz, 4H); ESI-MS observed *m/z* 468.65 ([*t*,*t*-**G**·Zn^{II}_2·**L3**]$^{4+}$).

Synthesis of [*t*,*t*-G·Fe^{II}_2·L3](PF$_6$)$_4$

To a degassed chloroform solution of *t*,*t*-**G** (2.13 mg, 1.77 μmol) were added a methanol solution of $FeCl_2 \cdot 4H_2O$ (2.5 mM, 1.42 mL, 3.55 μmol) and then a chloroform solution of **L3** (1.0 mM, 1.77 mL, 1.77 μmol). To this were added a mixed solvent of chloroform/acetonitrile (2/1) and saturated aqueous $NaPF_6$. An organic layer was separated, dried over $MgSO_4$, and evaporated. The crude products were passed thought silica-gel column chromatography (eluent: acetonitrile/water/saturated KNO_3 (7/0.7/0.3)). The obtained purple fraction was washed with saturated saturated aqueous $NaPF_6$ and then water to give blue powder of [*t*,*t*-**G**·Fe_2·**L3**](PF$_6$)$_4$ (1.1 mg, 0.45 μmol, 26%).

[*t*,*t*-**G**·Fe^{II}_2·**L3**](PF$_6$)$_4$: blue powder; ^{1}H NMR (600 MHz, CD_3CN) δ 1.01 (t, *J* = 7.0 Hz, 6H), 1.42-1.48 (m, 8H), 1.61 (quin, *J* = 7.6 Hz, 4H), 1.76 (quin, *J* = 7.6 Hz, 4H), 2.10-2.20 (m, 4H), 4.74 (t, *J* = 7.6 Hz, 4H), 5.08 (s, 8H), 6.73 (d, *J* = 8.6 Hz, 8H), 6.94 (s, 4H), 7.44 (d, *J* = 5.4 Hz, 4H), 7.48 (dd, *J* = 7.3 Hz, 5.4 Hz, 4H), 7.91 (dd, *J* = 8.3 Hz, 4H), 8.22 (dd, *J* = 7.7 Hz, 7.3 Hz, 4H), 8.47 (s, 4H), 8.61 (d, *J* = 8.3 Hz, 4H), 8.65 (s, 4H), 9.08 (d, *J* = 7.7Hz, 4H); ESI-MS observed *m/z* 463.6561 ([*t*,*t*-**G**·Fe^{II}_2·**L3**]$^{4+}$) calcd for [$C_{106}H_{94}N_{20}O_6Fe_2$]$^{4+}$ 463.6588.

Synthesis of [*t*,*t*-G·Fe^{II}_2·(L4)$_2$](PF$_6$)$_4$

To a degassed chloroform solution of *t*,*t*-**G** (0.50 mM, 500 μL, 0.25 μmol) were added a methanol solution of $FeCl_2 \cdot 4H_2O$ (2.5 mM, 200 μL, 0.50 μmol) and then a chloroform solution of **L4** (2.0 mM, 250 μL, 0.50 μmol). To this were added a mixed solvent of chloroform/acetonitrile (2/1) and saturated aqueous $NaPF_6$. An organic layer was separated, dried over $MgSO_4$, and evaporated. The crude products were passed thought silica-gel column chromatography (eluent: acetonitrile/water/saturated KNO_3 (7/0.7/0.3)). The obtained purple fraction was washed with saturated saturated aqueous $NaPF_6$ and then water to give purpled powder of [*t*,*t*-**1**·Fe_2·(**L4**)$_2$](PF$_6$)$_4$. The yield was not determined because of too small product to be weighted.

[*t*,*t*-**G**·Fe^{II}_2·(**L4**)$_2$](PF$_6$)$_4$: purple powder; ^{1}H NMR (600 MHz, CD_3CN) δ 0.91 (t, *J* = 6.5 Hz, 6H), 1.38-1.44 (m, 4H), 1.45-1.52 (m, 4H), 1.56 (quin, *J* = 6.5 Hz, 4H), 1.71 (quin, *J* = 6.5 Hz, 4H), 1.86 (quin, *J* = 6.5 Hz, 4H), 2.08 (quin, *J* = 6.5 Hz, 4H), 2.12 (s, 12H), 4.65 (t, *J* = 6.5 Hz, 4H), 5.00 (s, 8H), 6.74 (d, *J* = 8.8 Hz, 8H), 6.82 (s, 4H), 6.85 (s, 4H), 7.59 (d, *J* = 8.6 Hz, 4H), 7.85 (d, *J* = 8.8 Hz, 4H), 7.91 (d, *J* = 7.8 Hz, 4H), 8.02 (d, *J* =

8.6 Hz, 4H), 8.41 (m, 6H), 8.48 (d, J = 7.8 Hz, 4H), 8.49 (s, 4H); ESI-MS observed *m/z* 458.1727 ([*t*,*t*-**G**·Fe^{II}_2·(**L4**)$_2$]$^{4+}$) calcd for [$C_{108}H_{104}N_{16}O_6Fe_2$]$^{4+}$ 458.1753.

Synthesis of [*c*,*c*-G·Fe^{II}]$(PF_6)_2$

A degassed chloroform solution (5 mL) of *t*,*t*-**G** (9.70 mg, 8.09 μmol) was irradiated at 365 nm for 1 h. A degassed methanol solution (5 mL) of $FeCl_2·4H_2O$ (1.80 mg, 9.05 μmol) was then added, and the mixture was stirred for 30 min during irradiation. A mixed solvent of chloroform/acetonitrile (2:1) and saturated aqueous $NaPF_6$ were added to the reaction mixture. The organic layer was separated, dried over $MgSO_4$, and concentrated under reduced pressure to afford [*c*,*c*-**G**·Fe]$(PF_6)_2$ as a purple powder (11.5 mg, 7.44 μmol, 92%).

[*c*,*c*-**G**·Fe^{II}]$(PF_6)_2$: yellow powder, mp > 300 °C; ^{1}H NMR (600 MHz, CD_3CN) δ 0.94 (t, J = 7.2 Hz, 6H), 1.32-1.43 (m, 8H), 1.54 (quin, J = 7.2 Hz, 4H), 1.69 (quin, J = 7.2 Hz, 4H), 4.61 (t, J = 7.2 Hz,.7.2 Hz, 4H), 4.90 (d, J = 15.0 Hz, 4H), 4.96 (d, J = 15.0 Hz, 4H), 6.53 (d, J = 9.1 Hz, 8H), 6.57 (d, J = 9.1 Hz, 8H), 7.00 (s, 4H), 7.83 (d, J = 8.0 Hz, 4H), 8.34 (d, J = 8.0 Hz, 4H), 8.44 (s, 4H); ESI-MS observed *m/z* 627.2556 ([*c*,*c*-**G**·Fe^{II}]$^{2+}$) calcd for [$C_{74}H_{74}N_{10}O_6Fe$]$^{2+}$ 627.2571.

(3) 1D NMR spectra

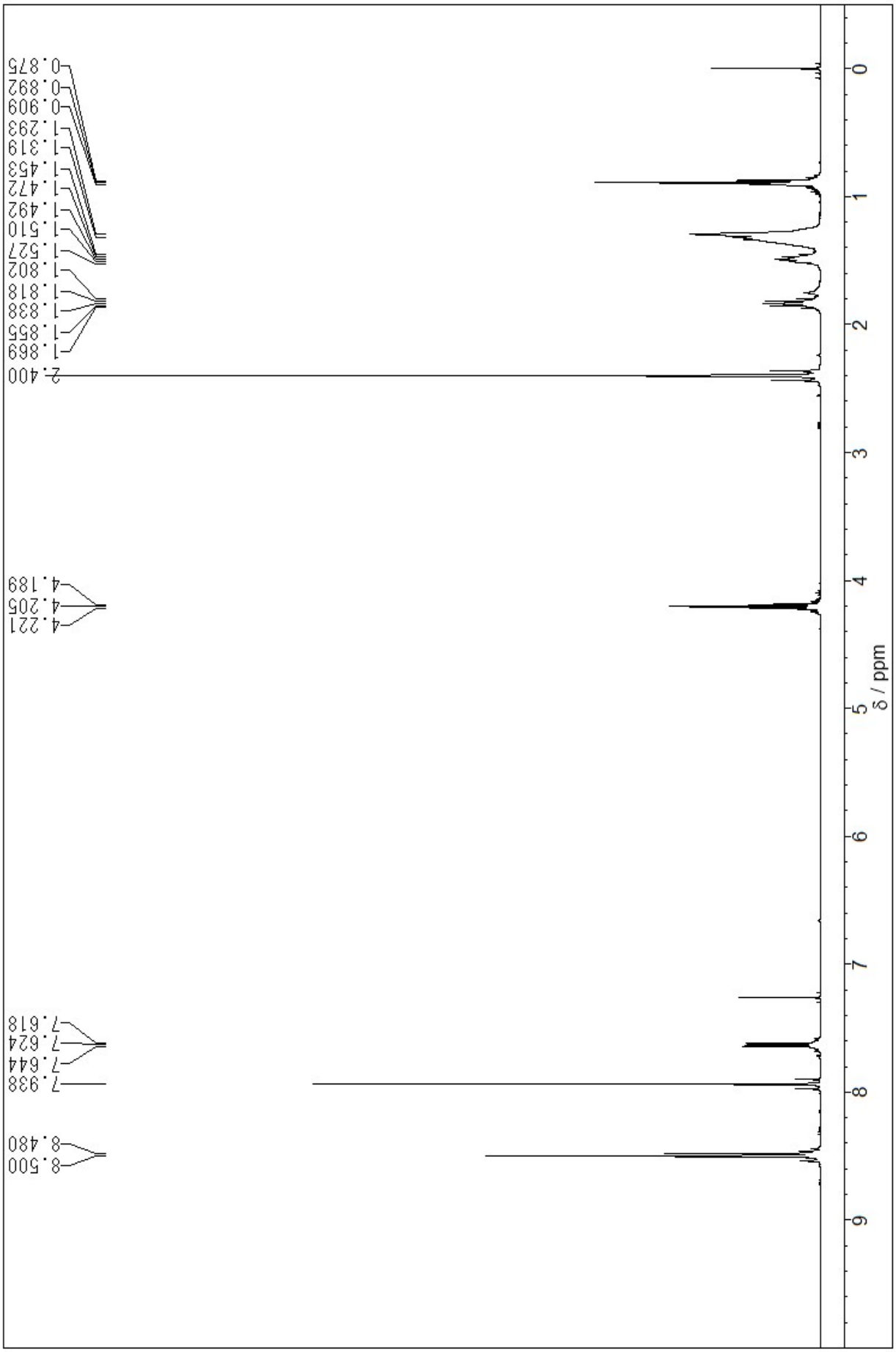

Figure S1. ^{1}H NMR spectrum of **6** (600 MHz, $CDCl_3$).

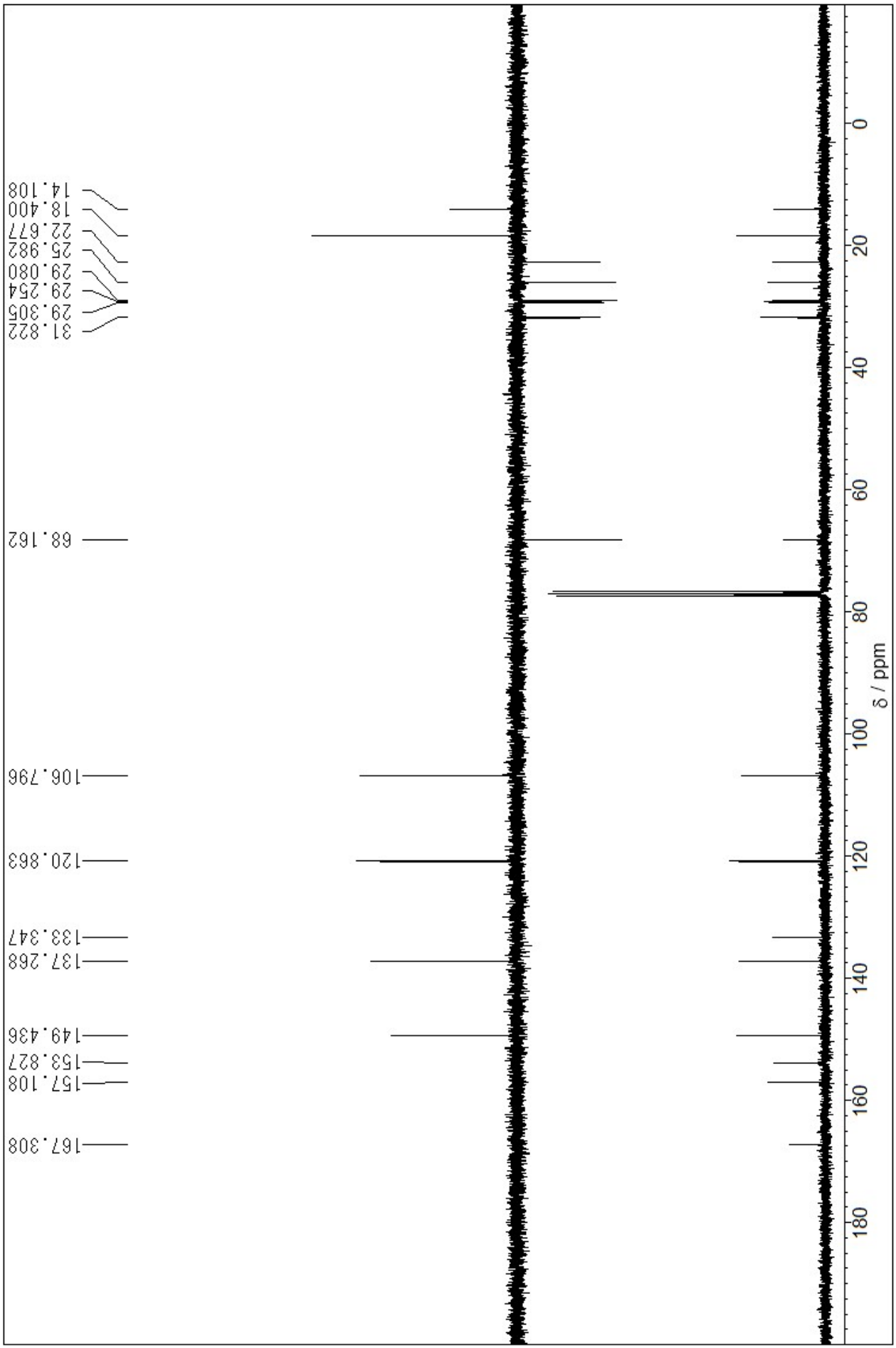

Figure S2. Dept135 (top) and ^{13}C NMR (bottom) spectra of **6** (600 MHz, $CDCl_3$).

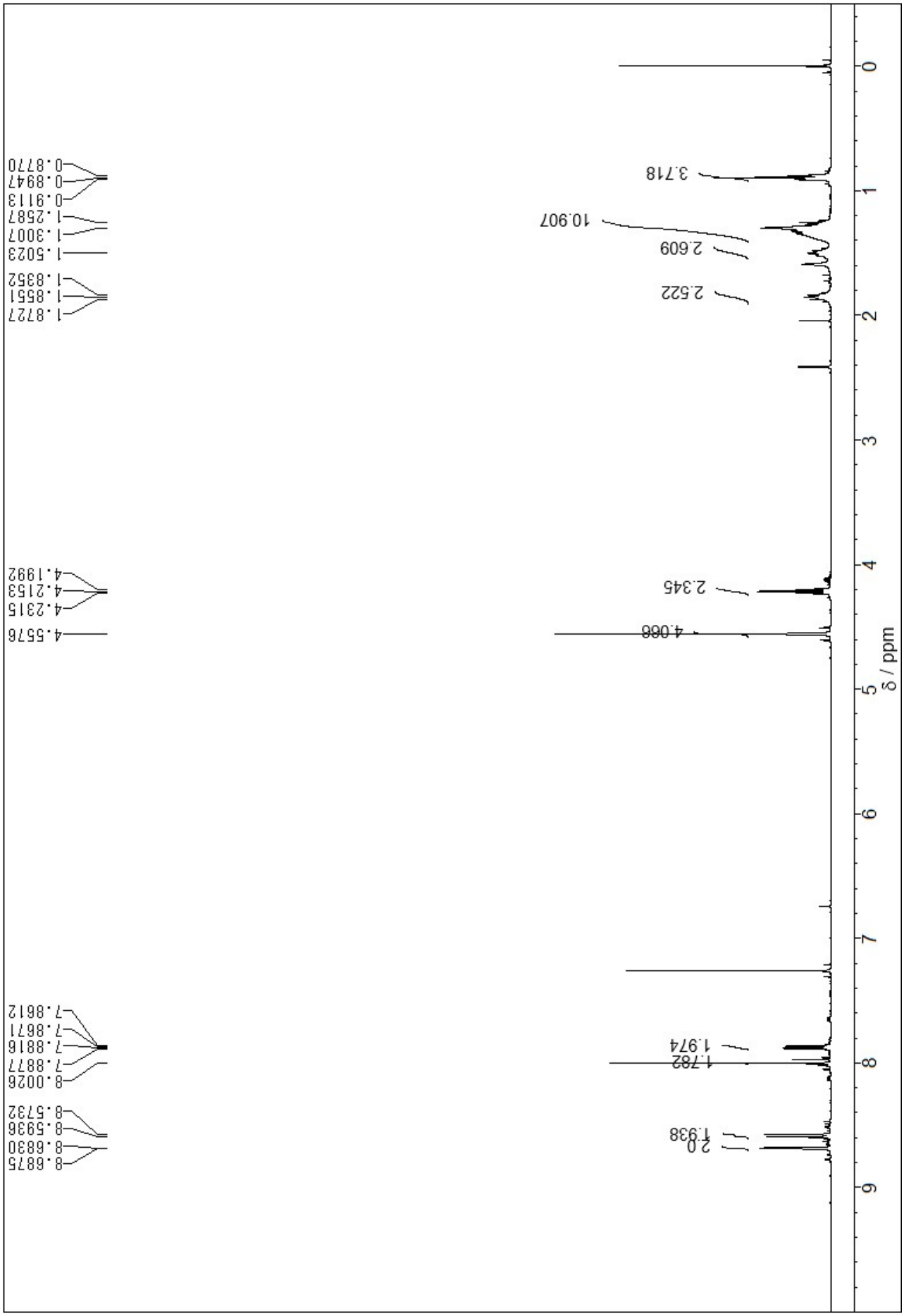

Figure S3. ^{1}H NMR spectrum of **1** (600 MHz, $CDCl_3$).

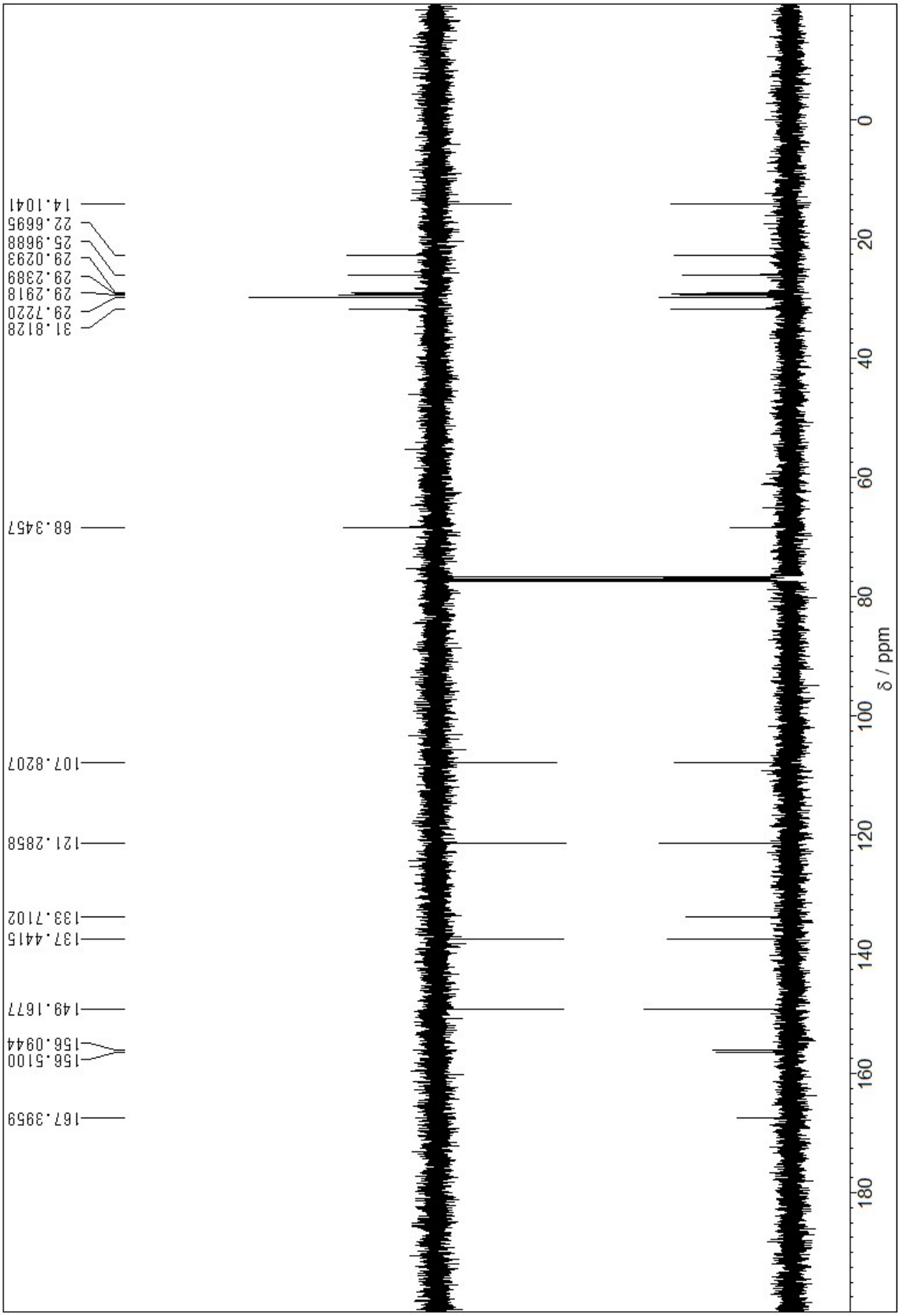

Figure S4. Dept135 (top) and ^{13}C NMR (bottom) spectra of **1** (600 MHz, $CDCl_3$).

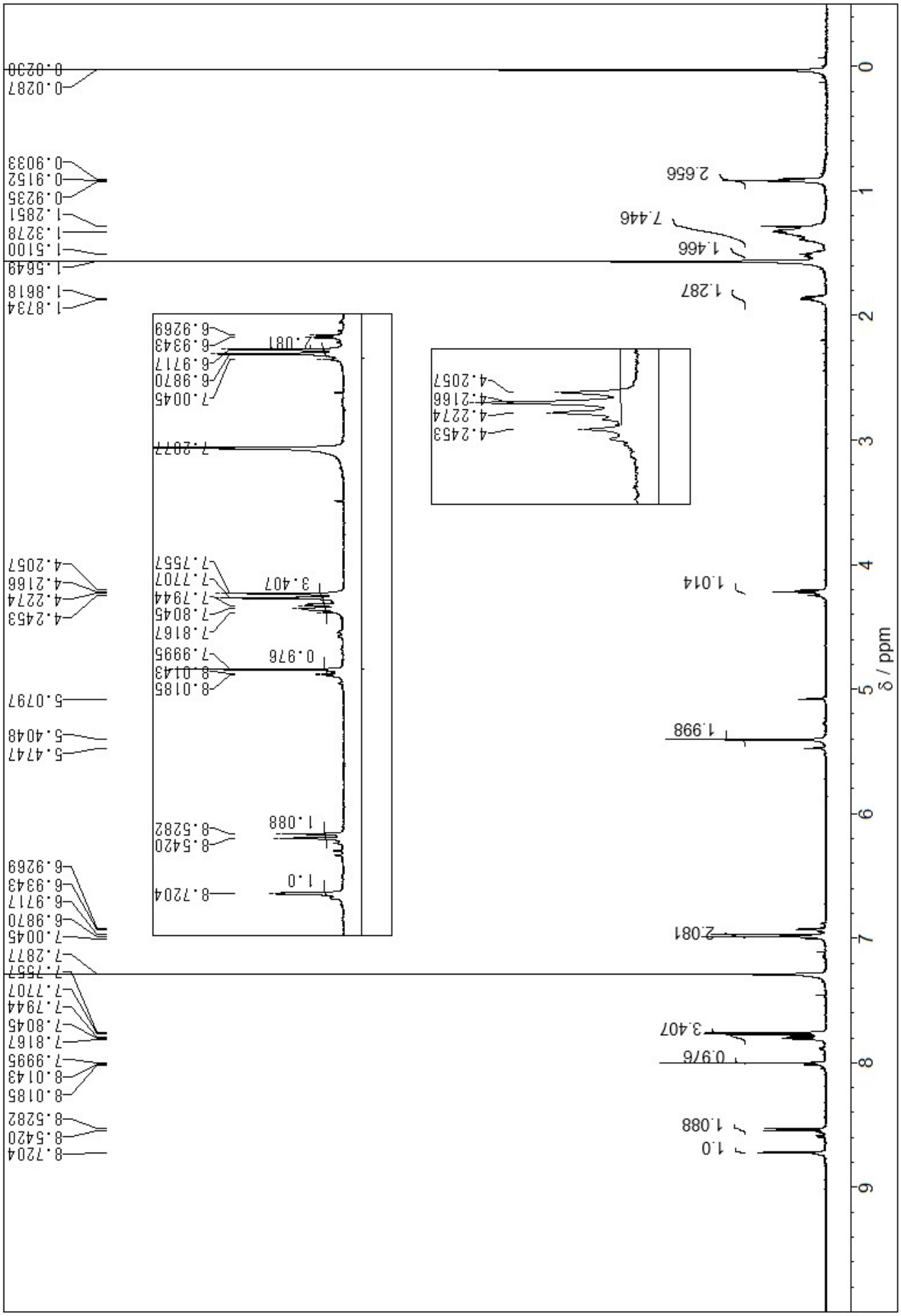

Figure S5. ^{1}H NMR spectra of *t,t*-**G** (600 MHz, $CDCl_3$). The *cis*-isomer of *t,t*-**G** was observed as a minor product.

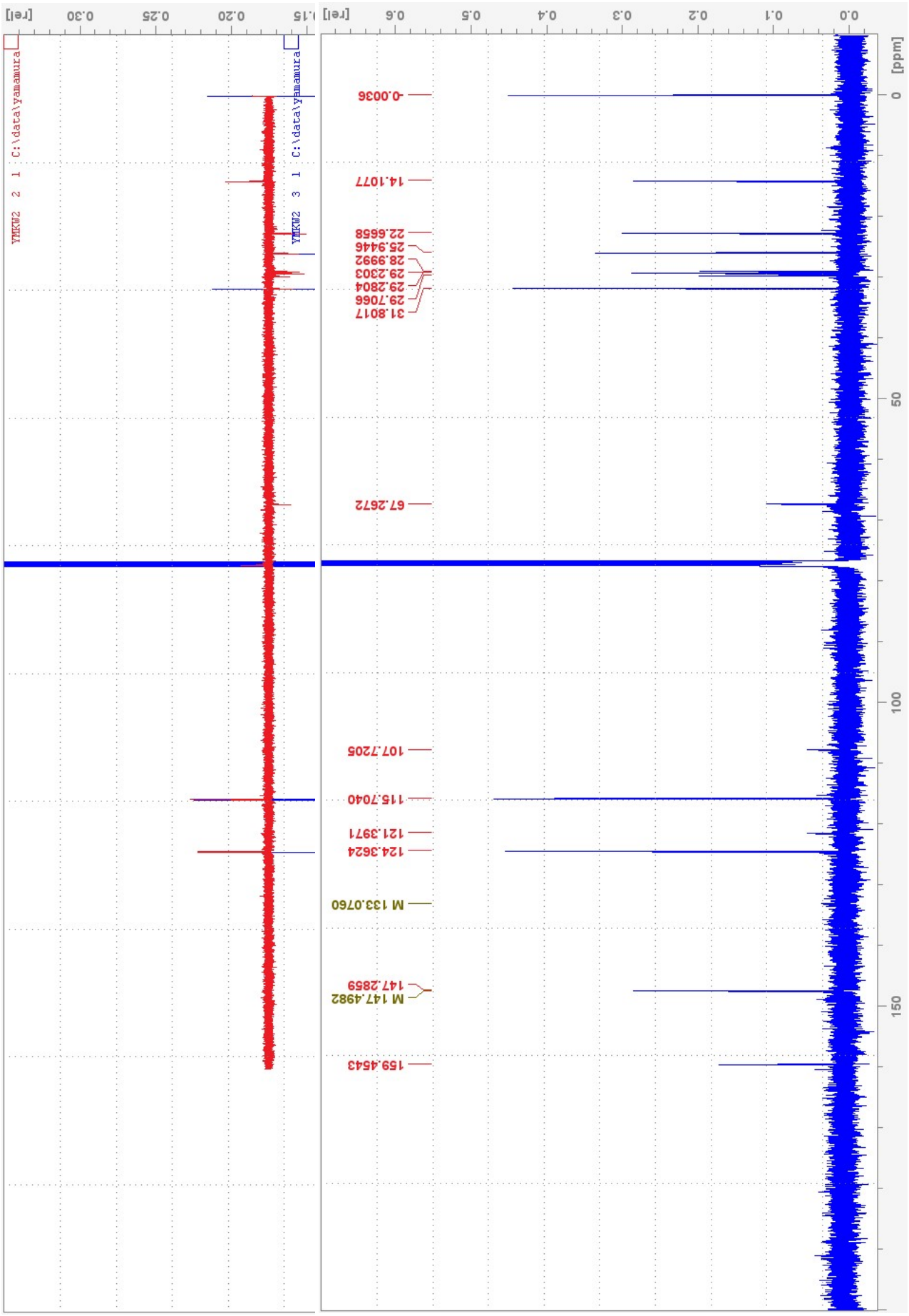

Figure S6. Dept135 (top) and ^{13}C NMR (bottom) spectra of *t,t*-**G** (100 MHz, $CDCl_3$). Carbon atoms in the terpyridine unit are broadening.

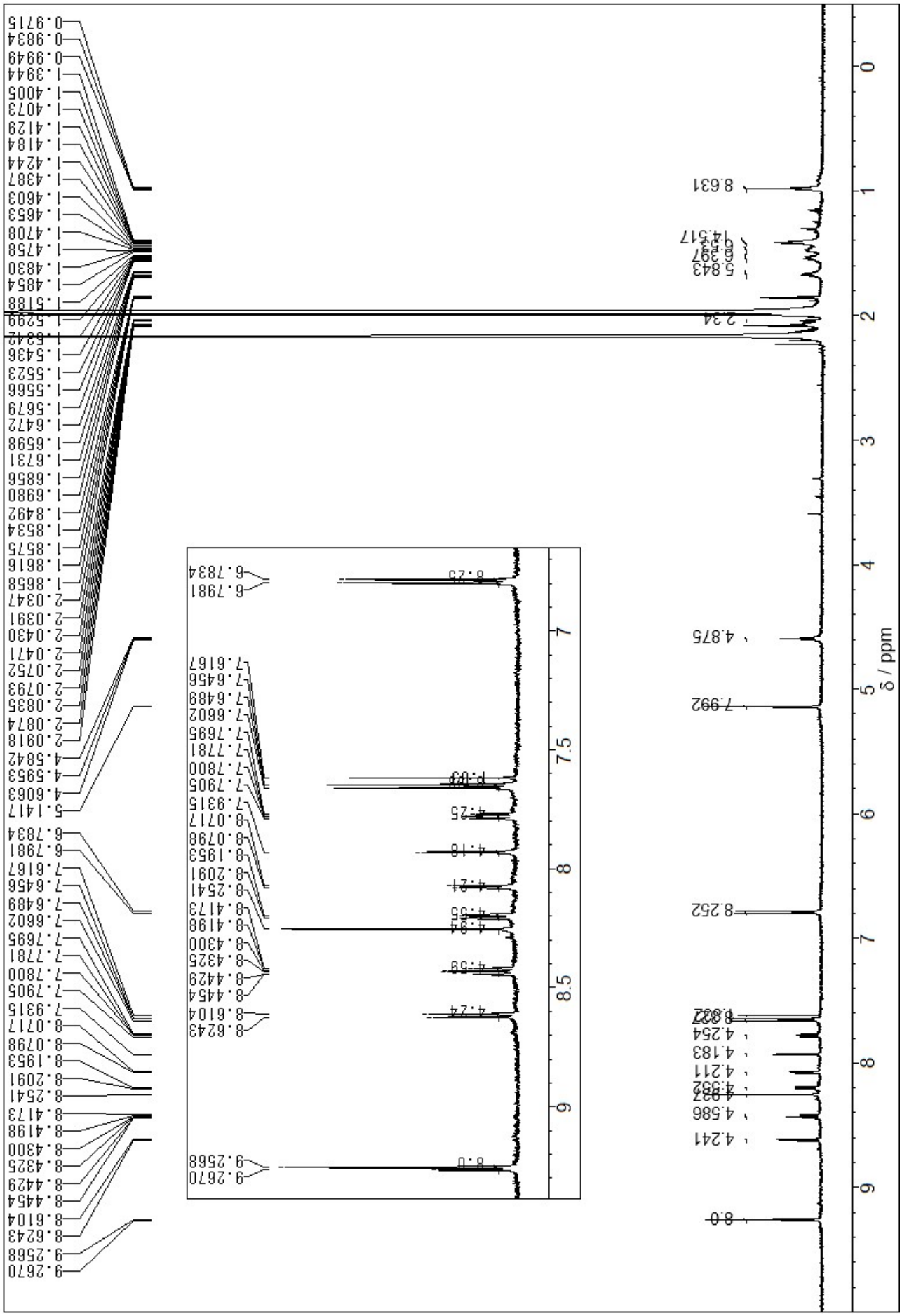

Figure S7. ^{1}H NMR spectra of [*t*,*t*-**G**·Zn^{II}_2·**L3**]$(ClO_4)_4$ (600 MHz, CD_3CN).

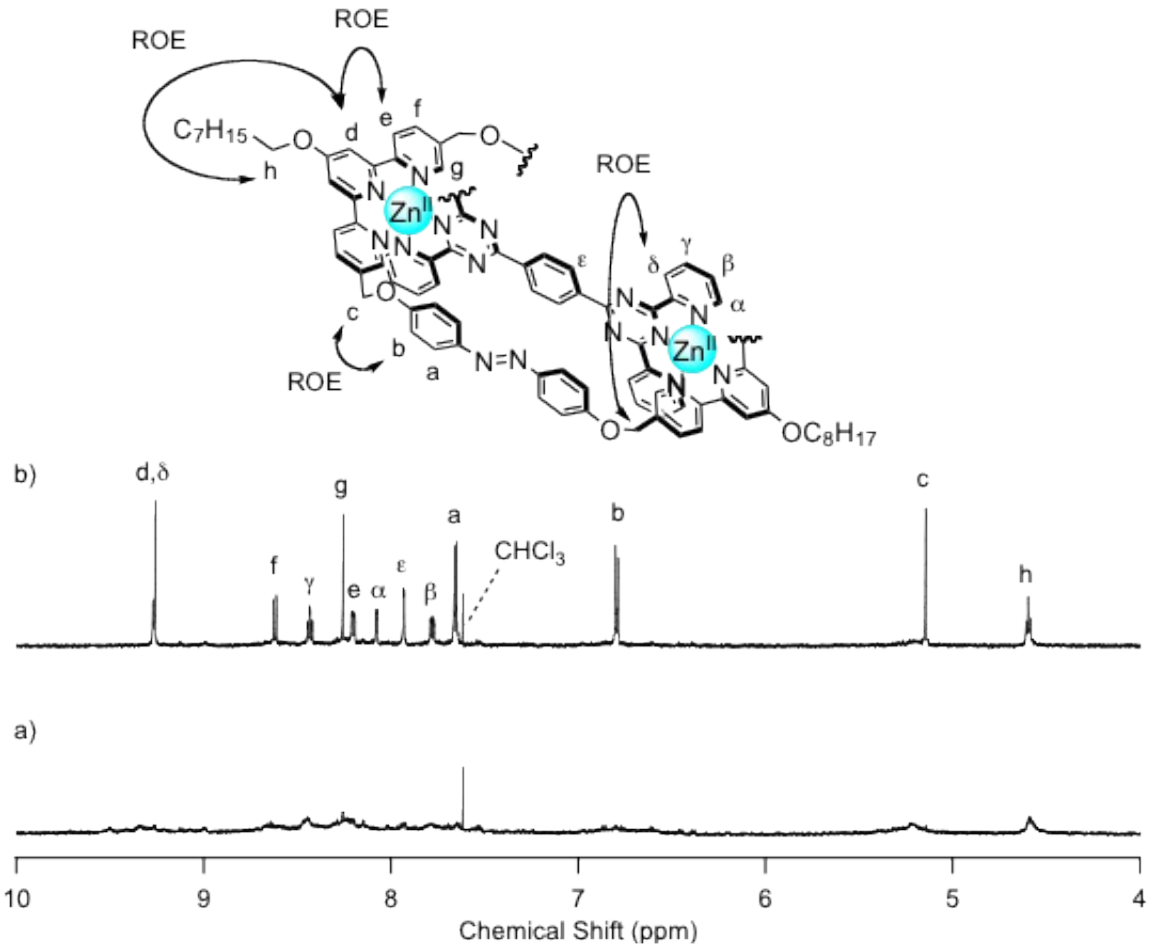

Figure S8. ^{1}H NMR spectra of [*t*,*t*-**G**·Zn^{II}_2·**L3**]$(ClO_4)_4$ (600 MHz, CD_3CN), a) before and b) after the addition of **L3**. Identification of [*t*,*t*-**G**·Zn^{II}_2·**L3**]$(ClO_4)_4$ by ROESY.

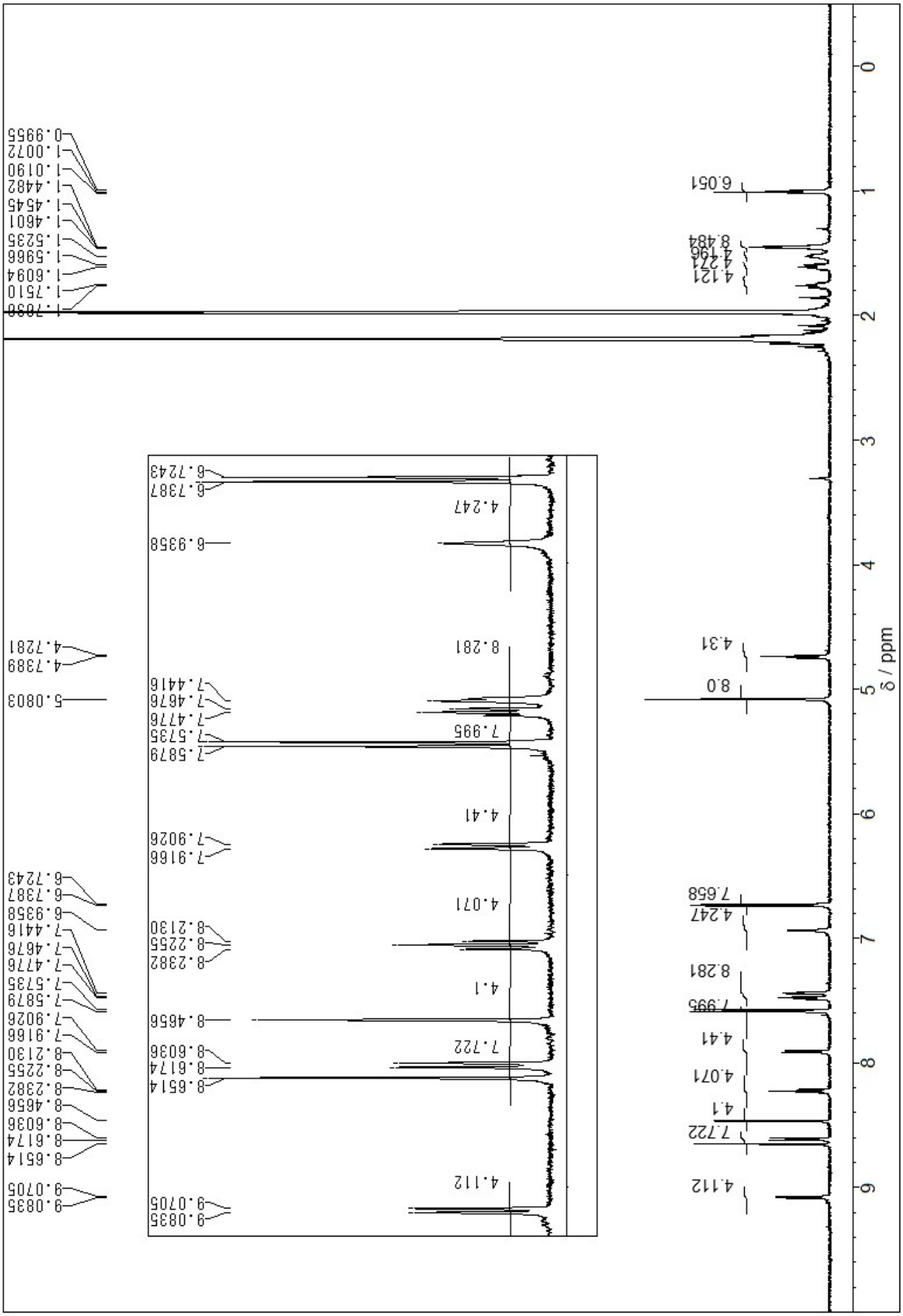

Figure S9. ^{1}H NMR spectra of [*t*,*t*-**G**·Fe^{II}_2·**L3**]$(PF_6)_4$ (600 MHz, CD_3CN).

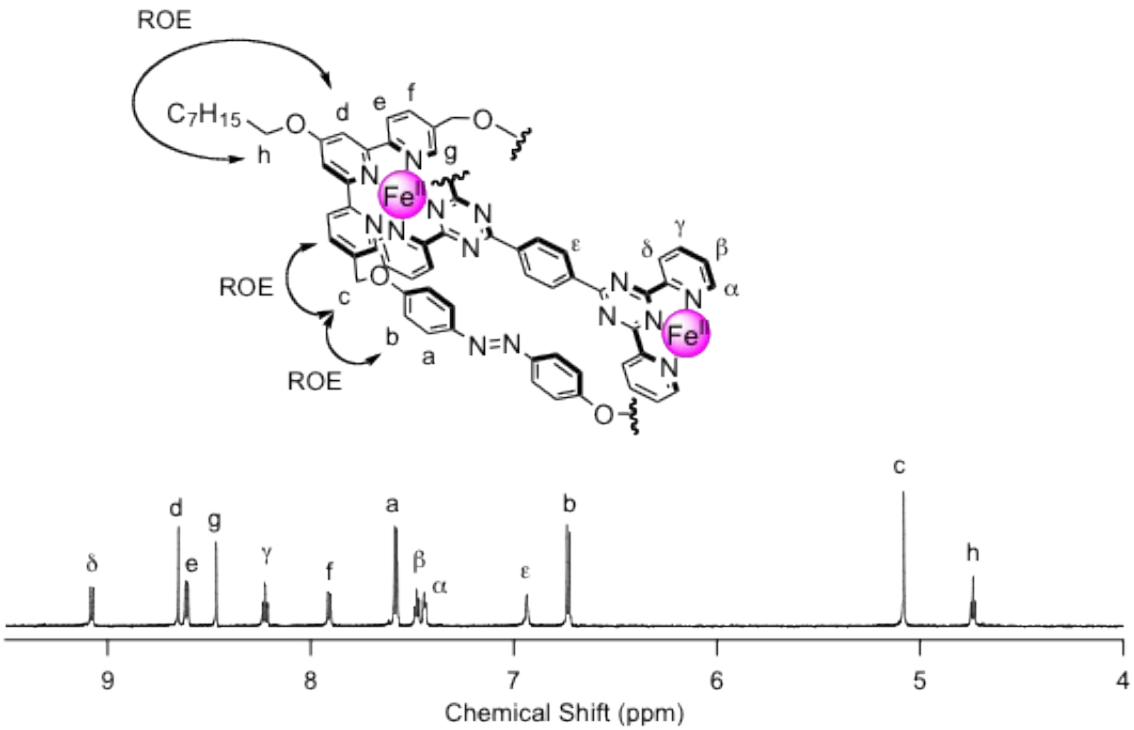

Figure S10. Identification of [*t*,*t*-**G**·Fe^{II}_2·**L3**]$(PF_6)_4$ by ROESY.

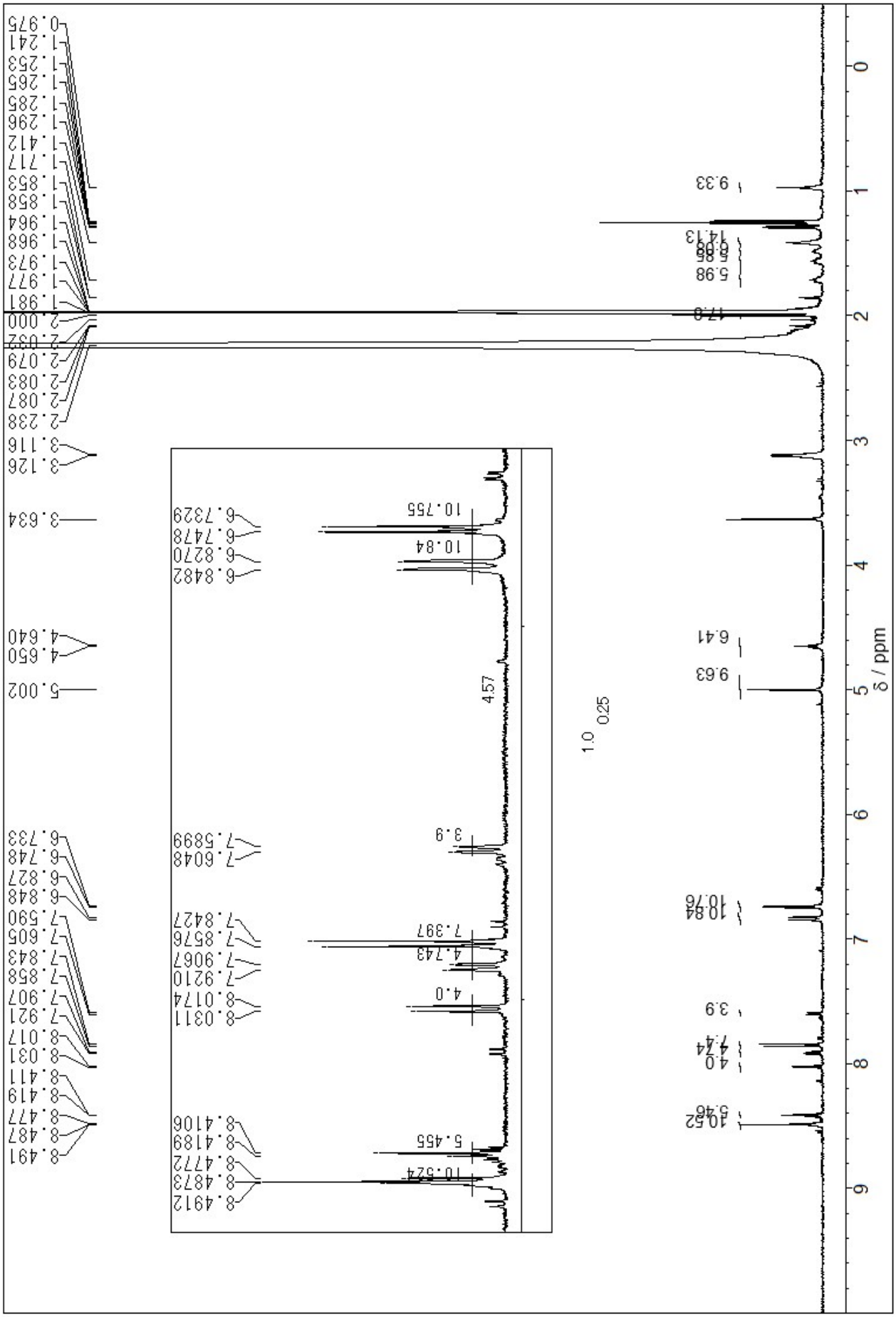

Figure S11. ^{1}H NMR spectra of [*t*,*t*-**G**·Fe^{II}_2·(**L4**)$_2$](PF$_6$)$_4$ (600 MHz, CD_3CN). The *cis*-isomer of [*t*,*t*-**G**·Fe^{II}_2·(**L4**)$_2$](PF$_6$)$_4$ was observed as a minor product.

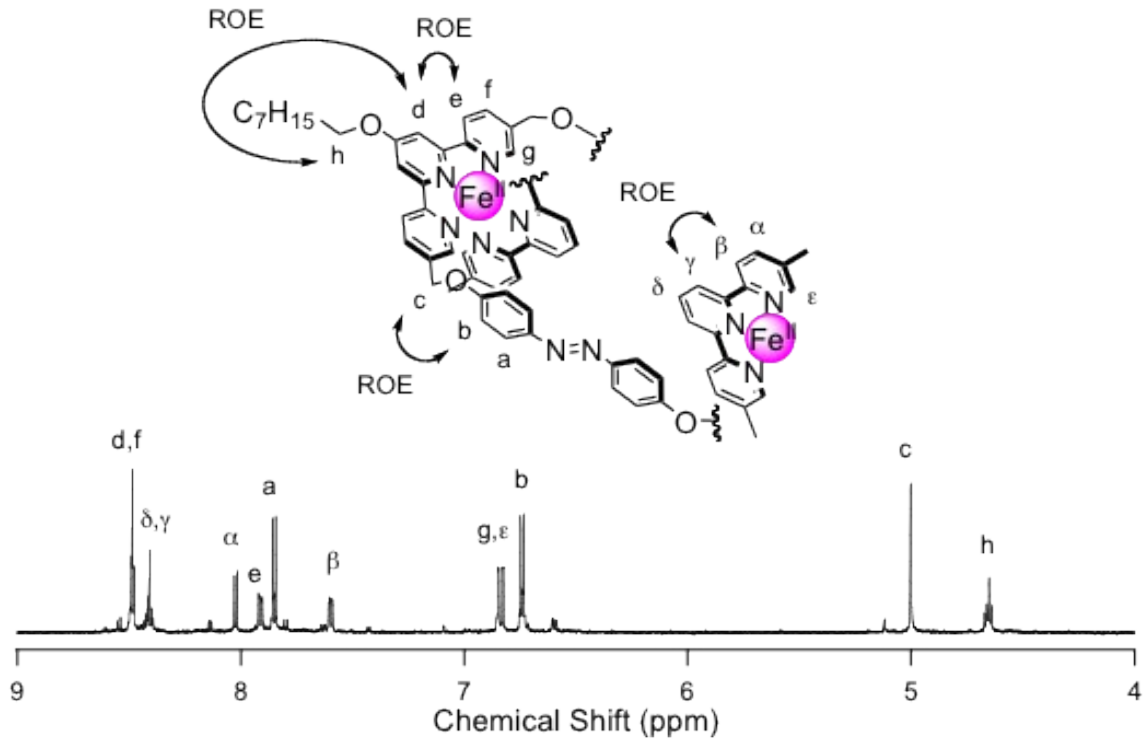

Figure S12. Identification of [*t*,*t*-**G**·Fe^{II}_2·(**L4**)$_2$]$(PF_6)_4$ by ROESY.

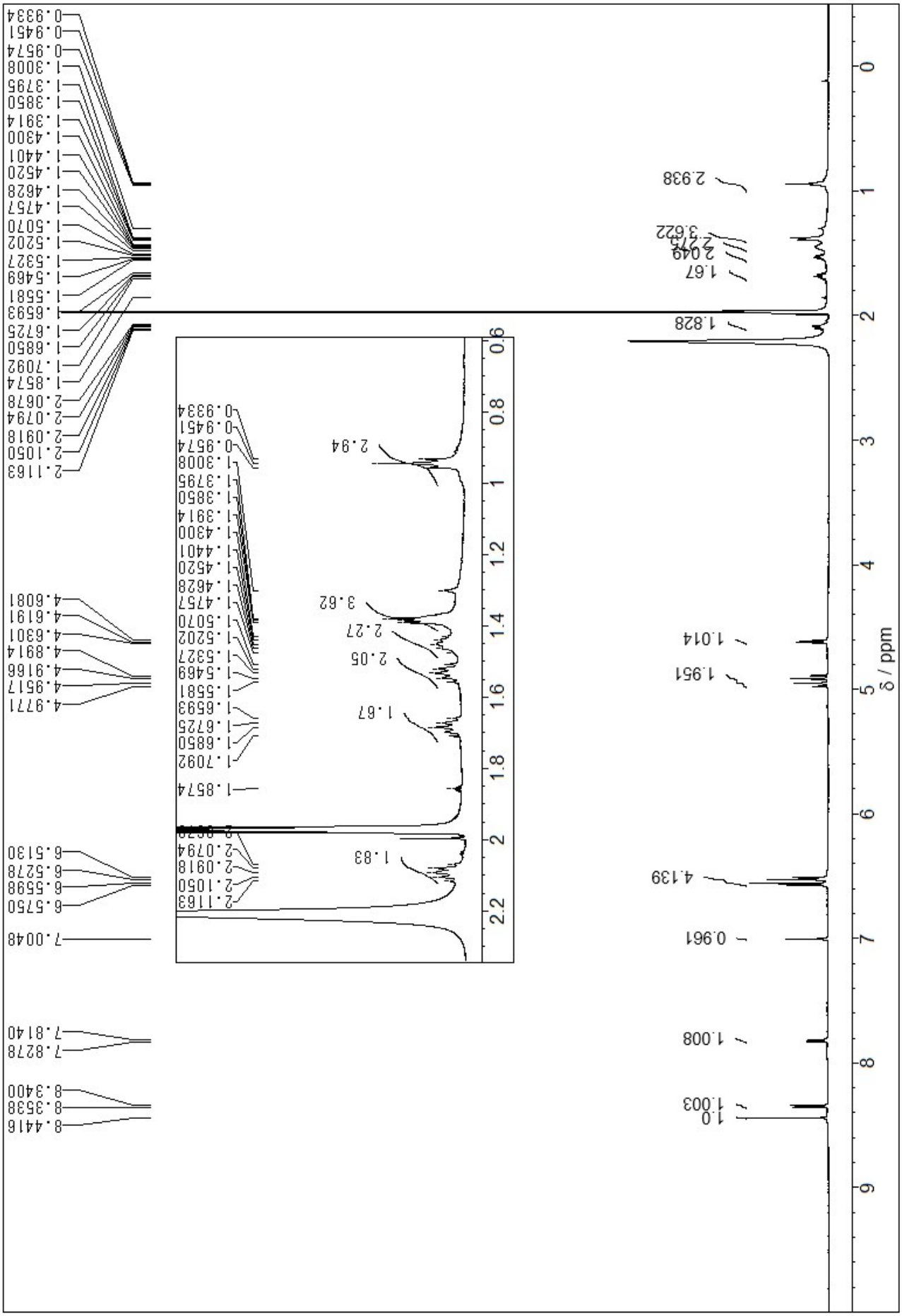

Figure S13. ^{1}H NMR spectra of [*c*,*c*-**G**·Fe^{II}](PF$_6$)$_2$ (600 MHz, CD$_3$CN).

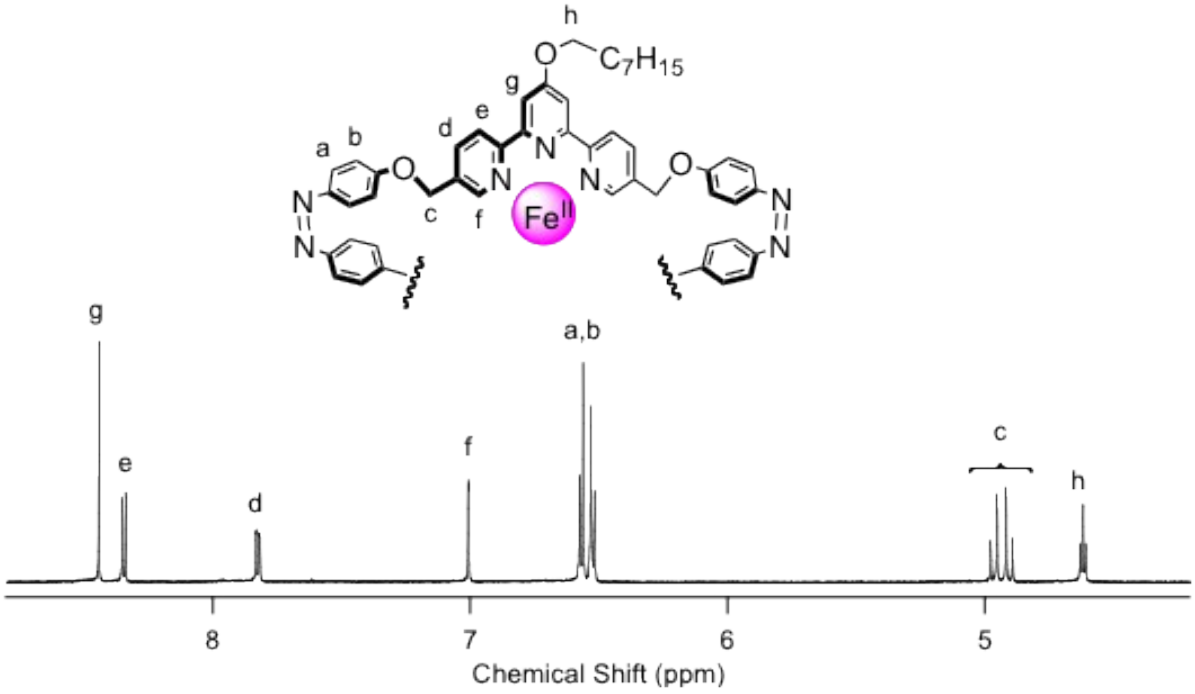

Figure S14. Identification of [*c*,*c*-**G**·Fe^{II}]$(PF_6)_2$ by ROESY.

(4) 2D diffusion-ordered NMR spectra (DOSY)

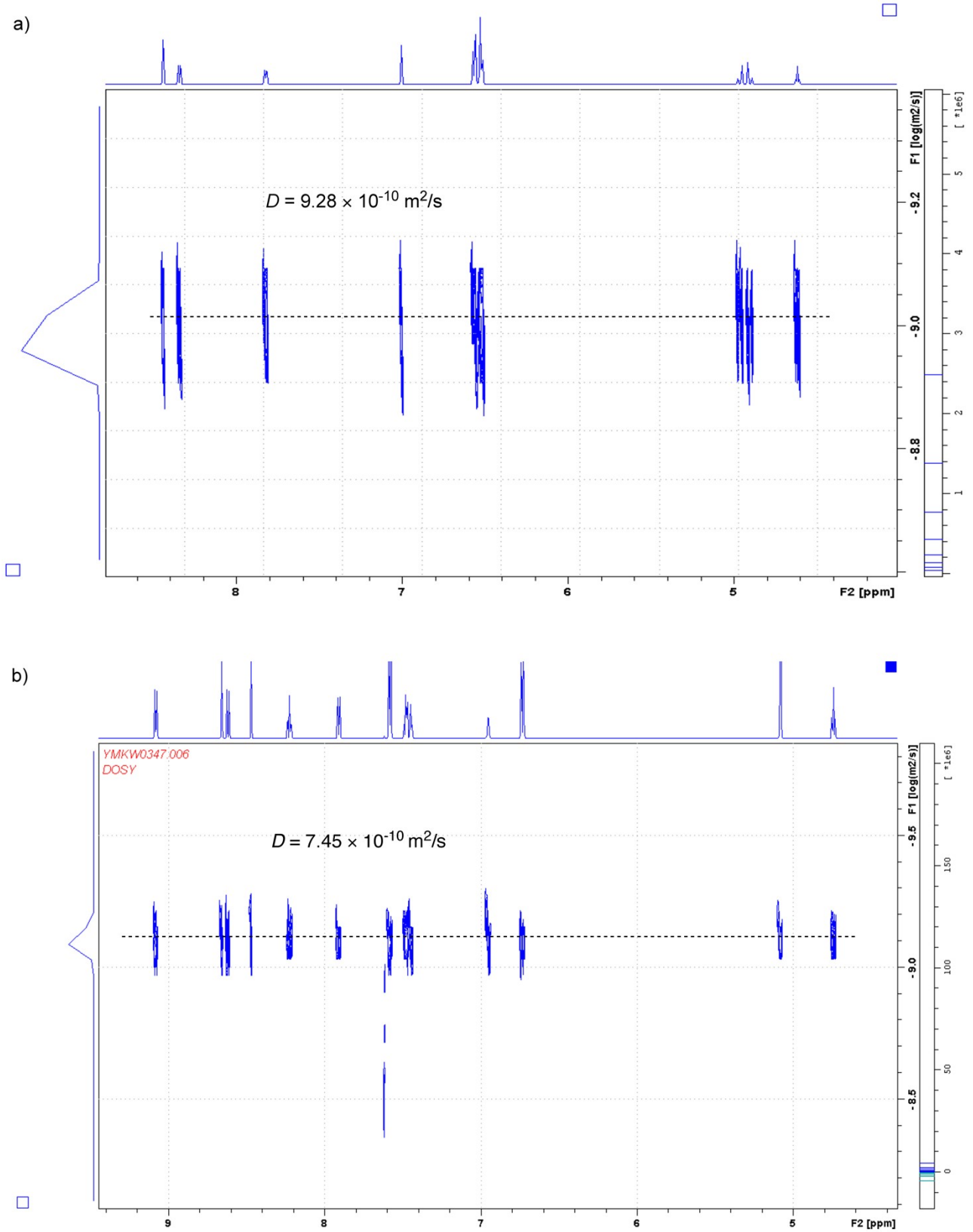

Figure S15. ^{1}H DOSY of (a) [*c*,*c*-**G**·Fe^{II}]$(PF_6)_2$ and (b) [*t*,*t*-**G**·Fe^{II}_2·**L3**]$(PF_6)_4$ (600 MHz, CD_3CN, 300 K).

(5) ESI mass spectra

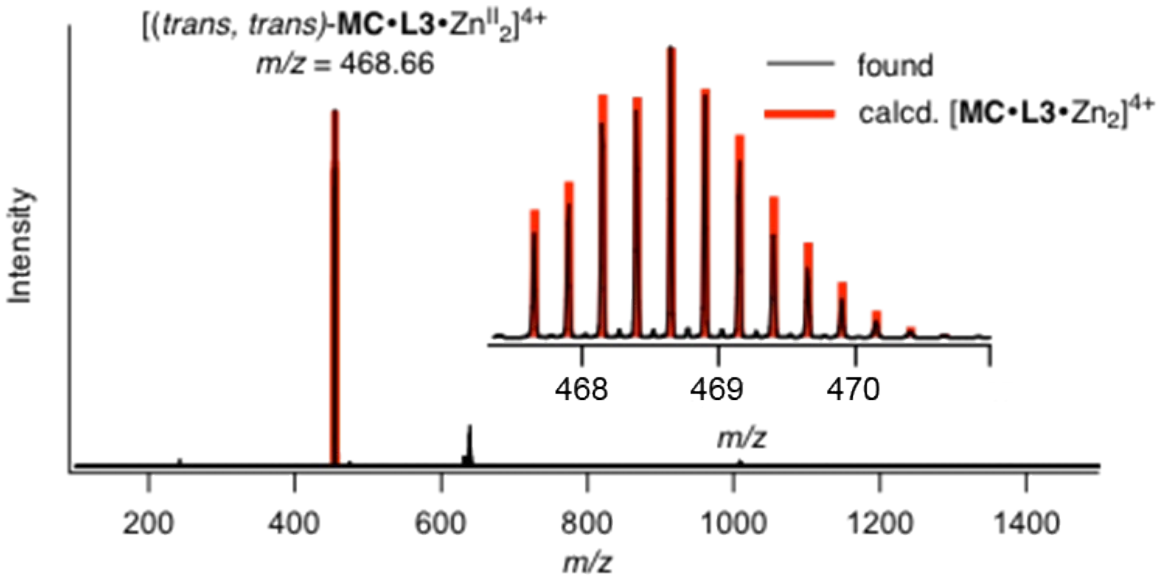

Figure S16. ESI-TOF MS of [*t*,*t*-**G**·Zn$^{II}_2$·**L3**](ClO$_4$)$_4$.

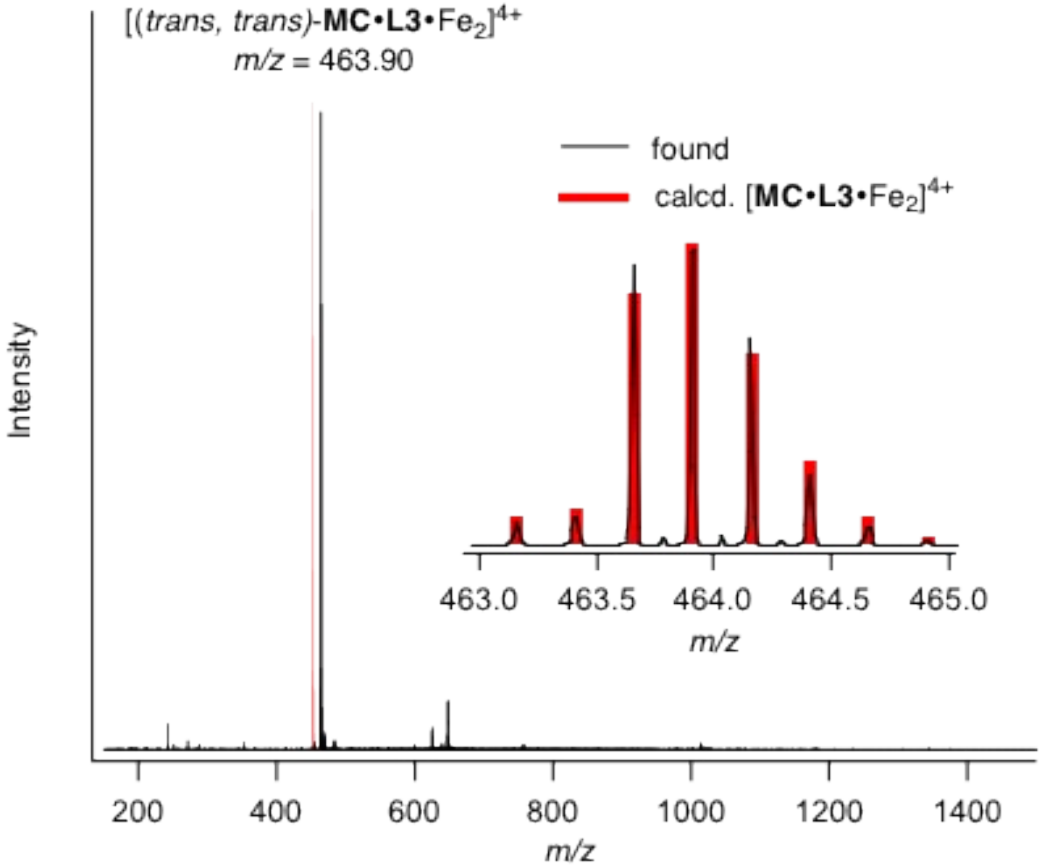

Figure S17. ESI-TOF MS of [*t*,*t*-**G**·Fe$^{II}_2$·**L3**](PF$_6$)$_4$.

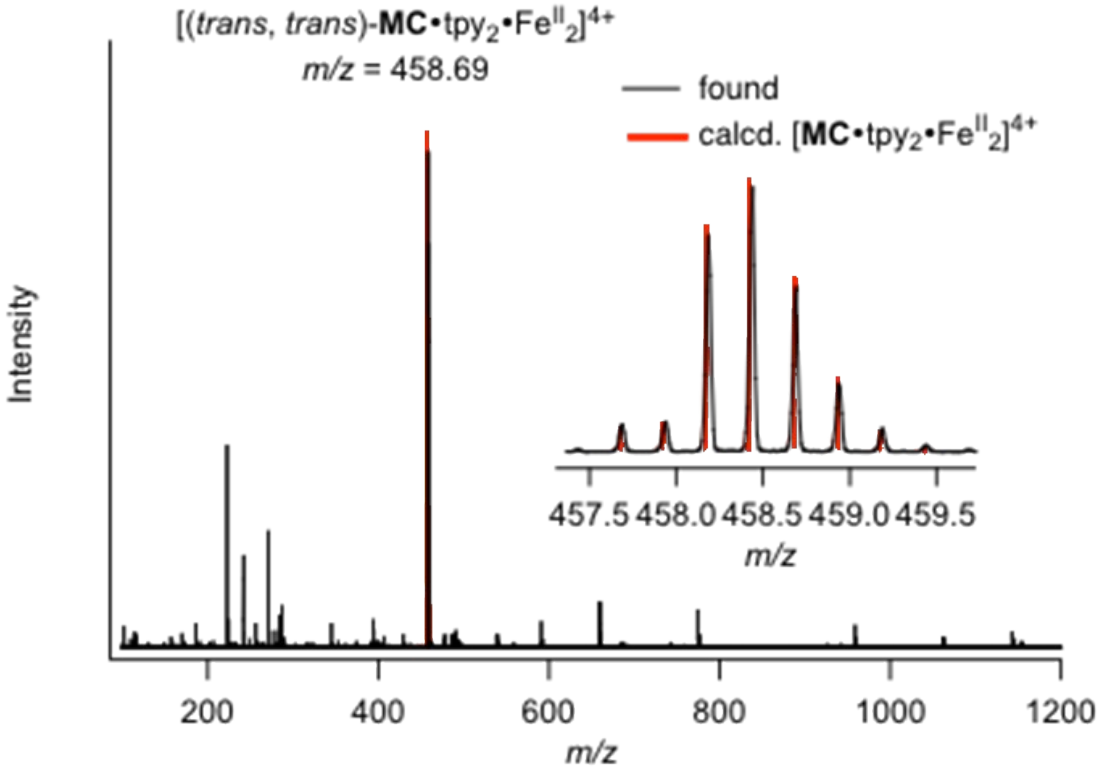

Figure S18. ESI-TOF MS of [*t*,*t*-**G**·Fe^{II}_2·(**L4**)$_2$]$(PF_6)_4$.

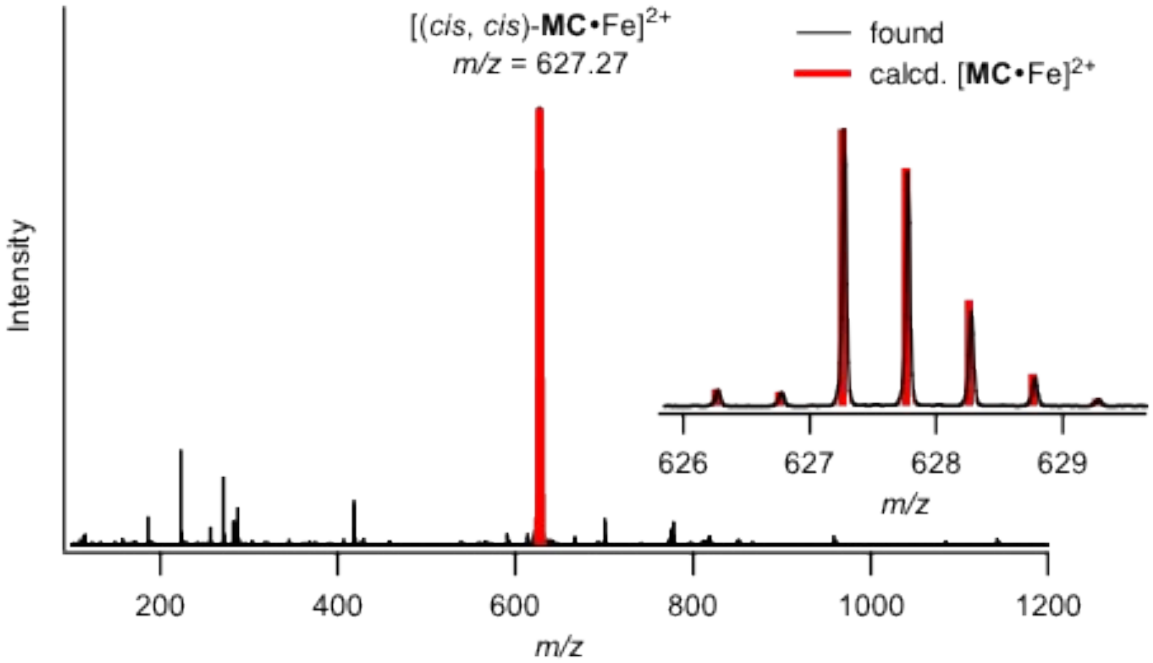

Figure S19. ESI-TOF MS of [*c*,*c*-**G**·Fe^{II}]$(PF_6)_2$.

(6) Complexation

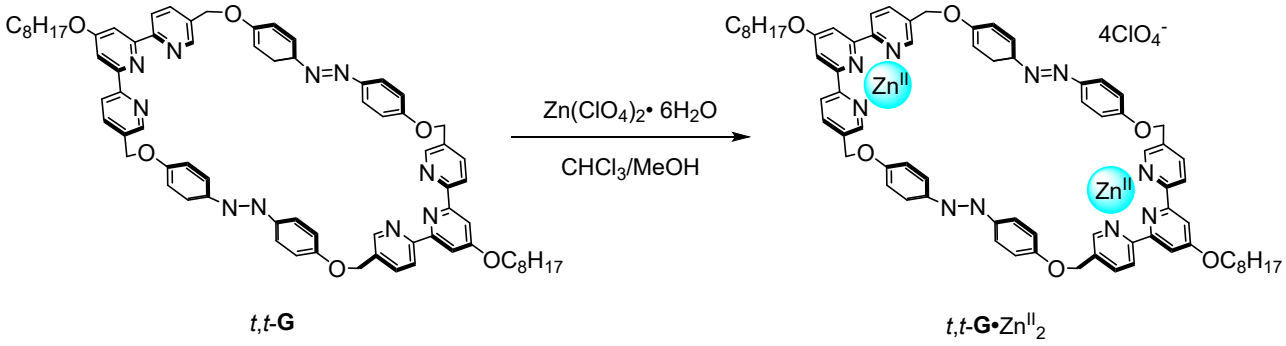

t,*t*-**G** *t*,*t*-**G**•Zn^{II}_2

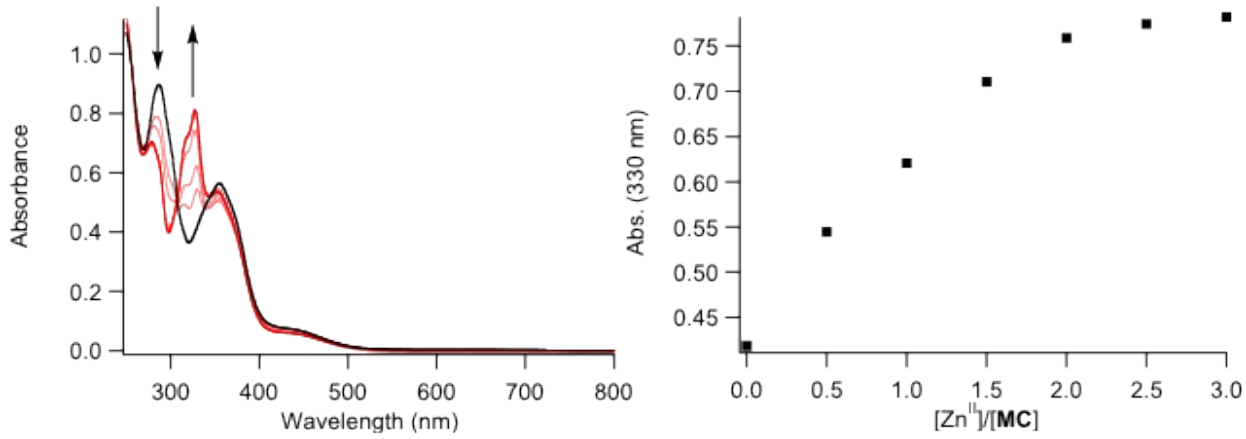

Figure S20. UV-vis spectral changes of *t*,*t*-**G** upon addition of $Zn(ClO_4)_2 \cdot 6H_2O$, $CHCl_3$/MeOH (1/1), 20 μM, l = 1 cm, $0 \leq [Zn^{II}]/[t,t\text{-}\mathbf{G}] \leq 3.0$

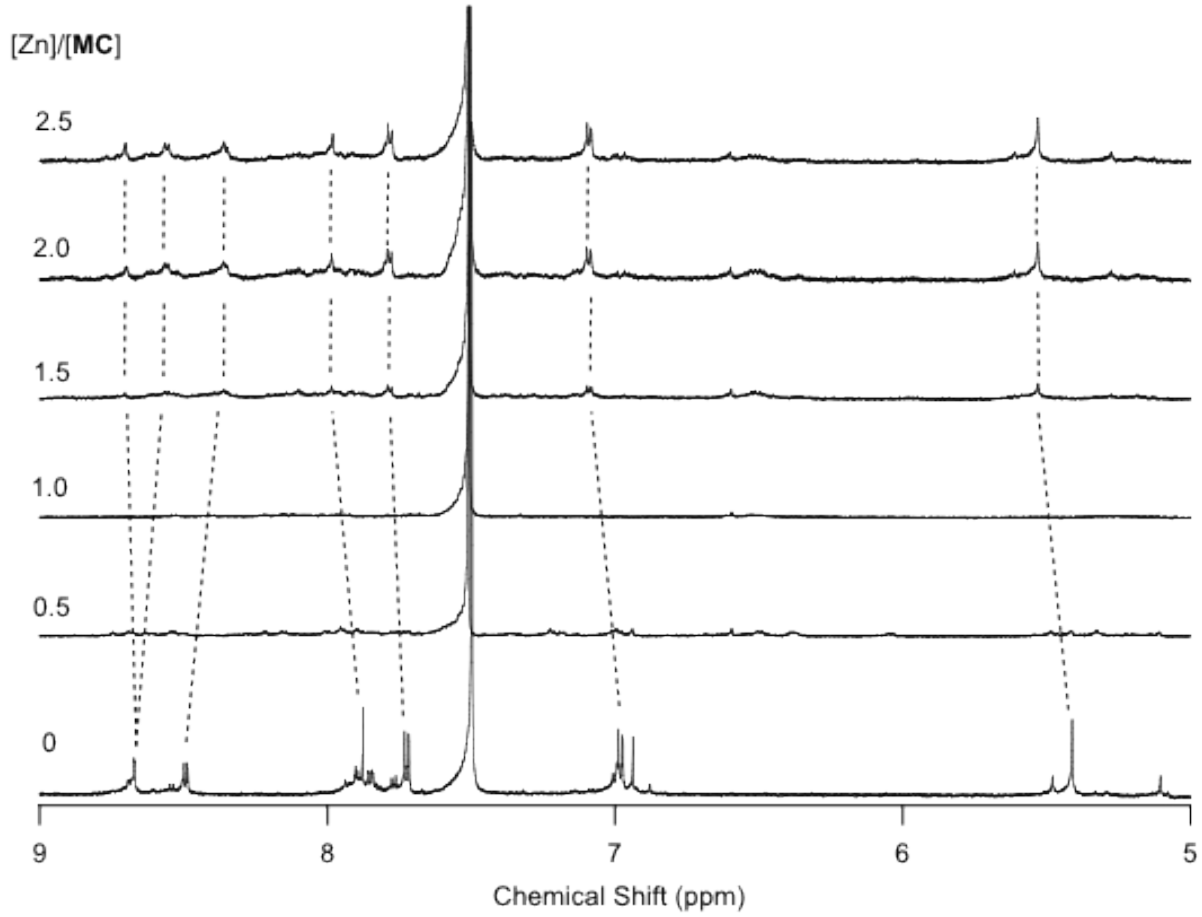

Figure S21. ^{1}H NMR spectral changes of *t*,*t*-**G** upon addition of $Zn(ClO_4)_2 \cdot 6H_2O$, $CDCl_3/CD_3CN$ (3/2), [*t*,*t*-**G**] = 100 μM, 600 MHz.

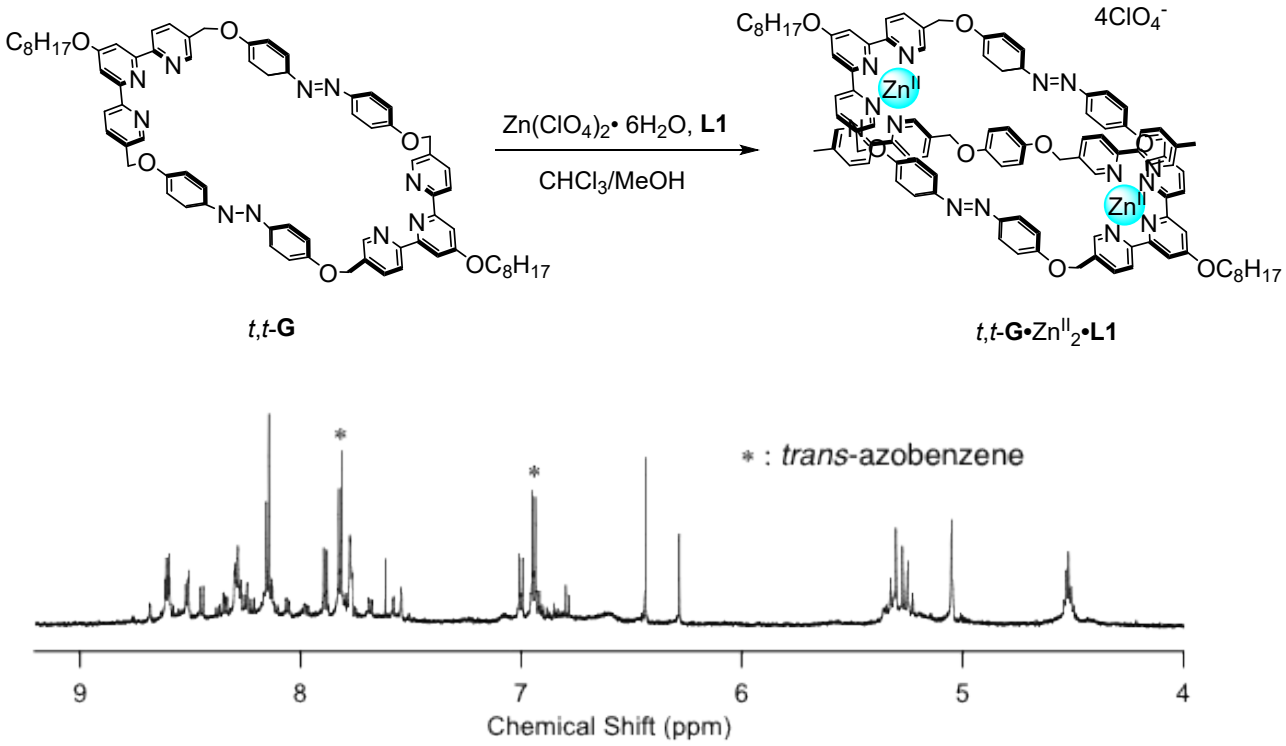

Figure S22. ^{1}H NMR spectrum (600 MHz, CD_3CN) of [*t*,*t*-**G**·Zn^{II}_2·**L1**]$(ClO_4)_4$.

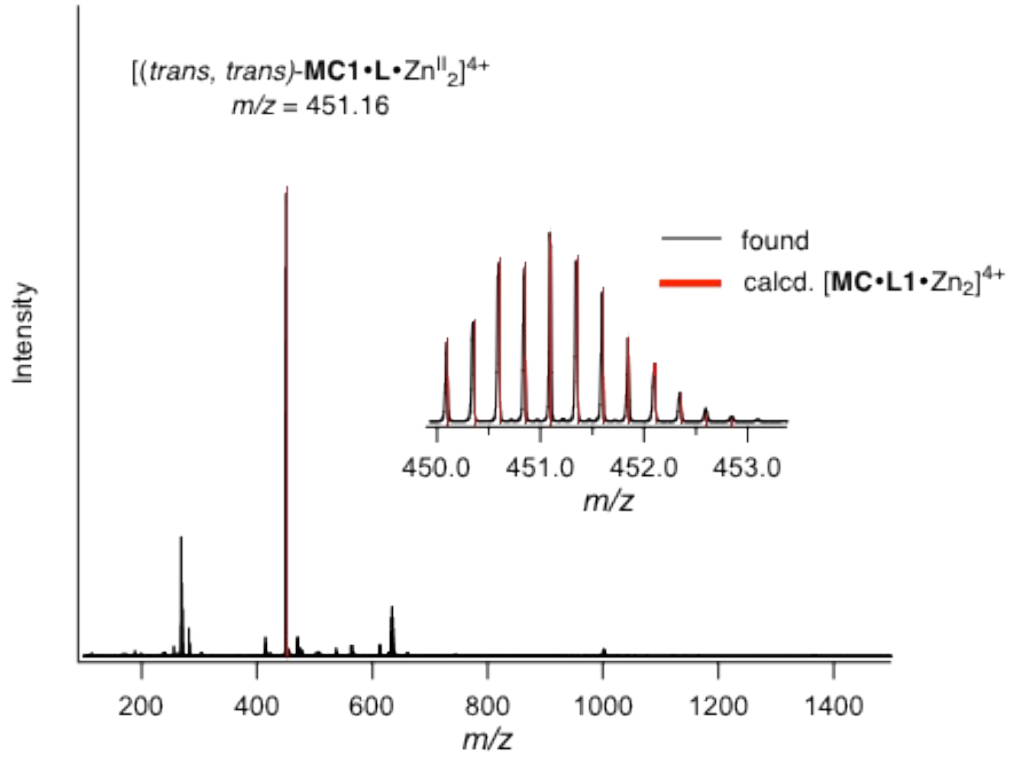

Figure S23. ESI-MS of *t*,*t*-**G**·Zn^{II}_2·**L1**.

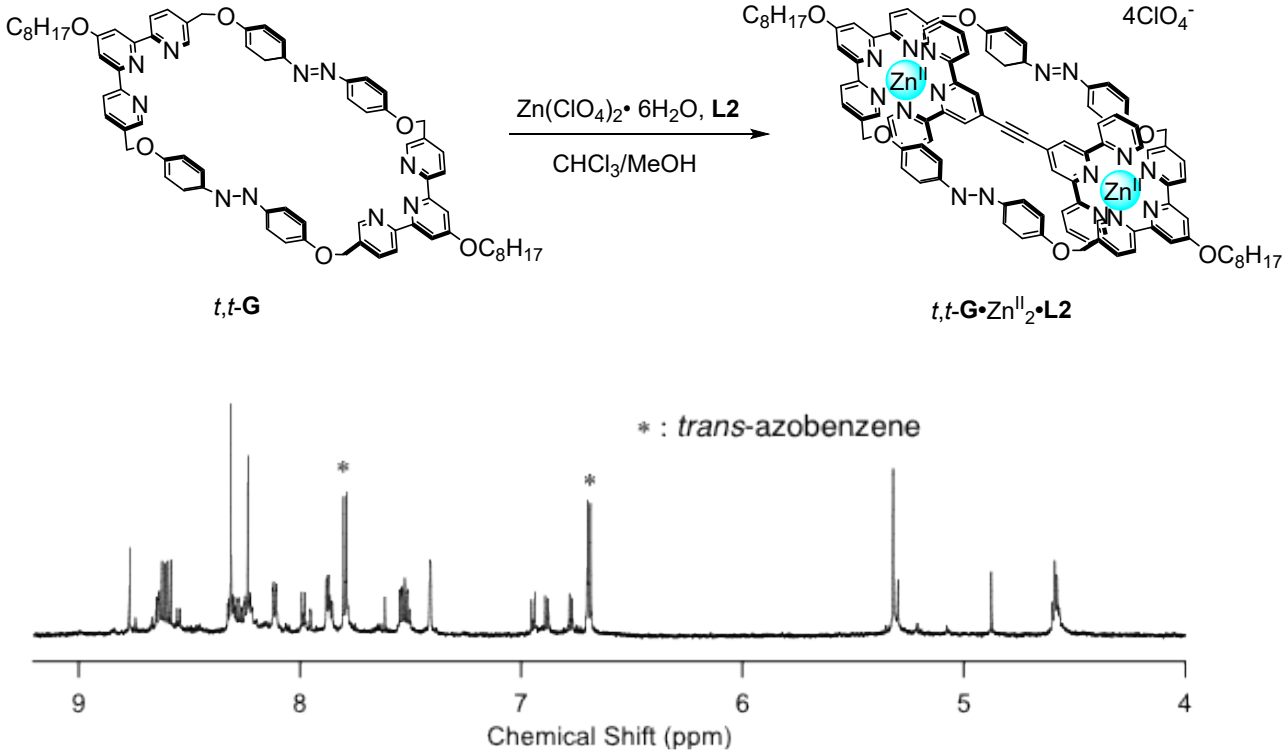

Figure S24. ^{1}H NMR spectrum (600 MHz, CD_3CN) of [*t,t*-**G**·Zn^{II}_2·**L2**]$(ClO_4)_4$.

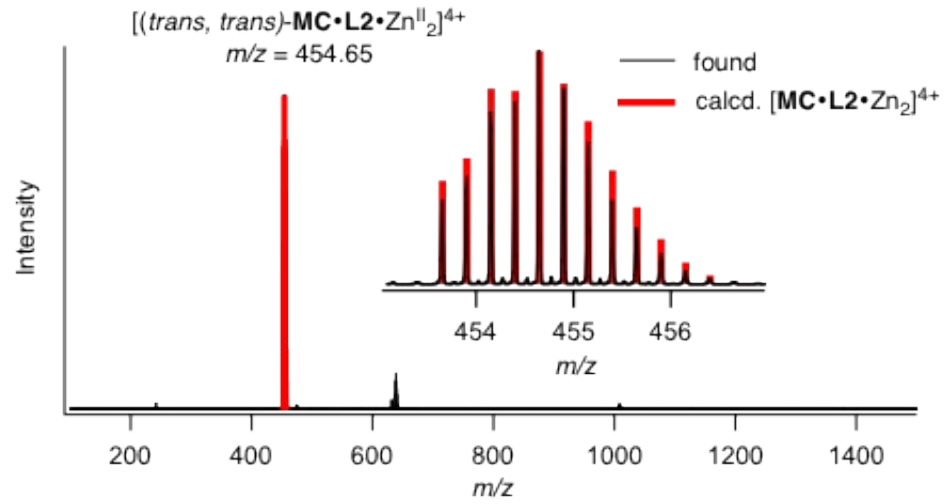

Figure S25. ESI-MS of *t,t*-**G**·Zn^{II}_2·**L2**.

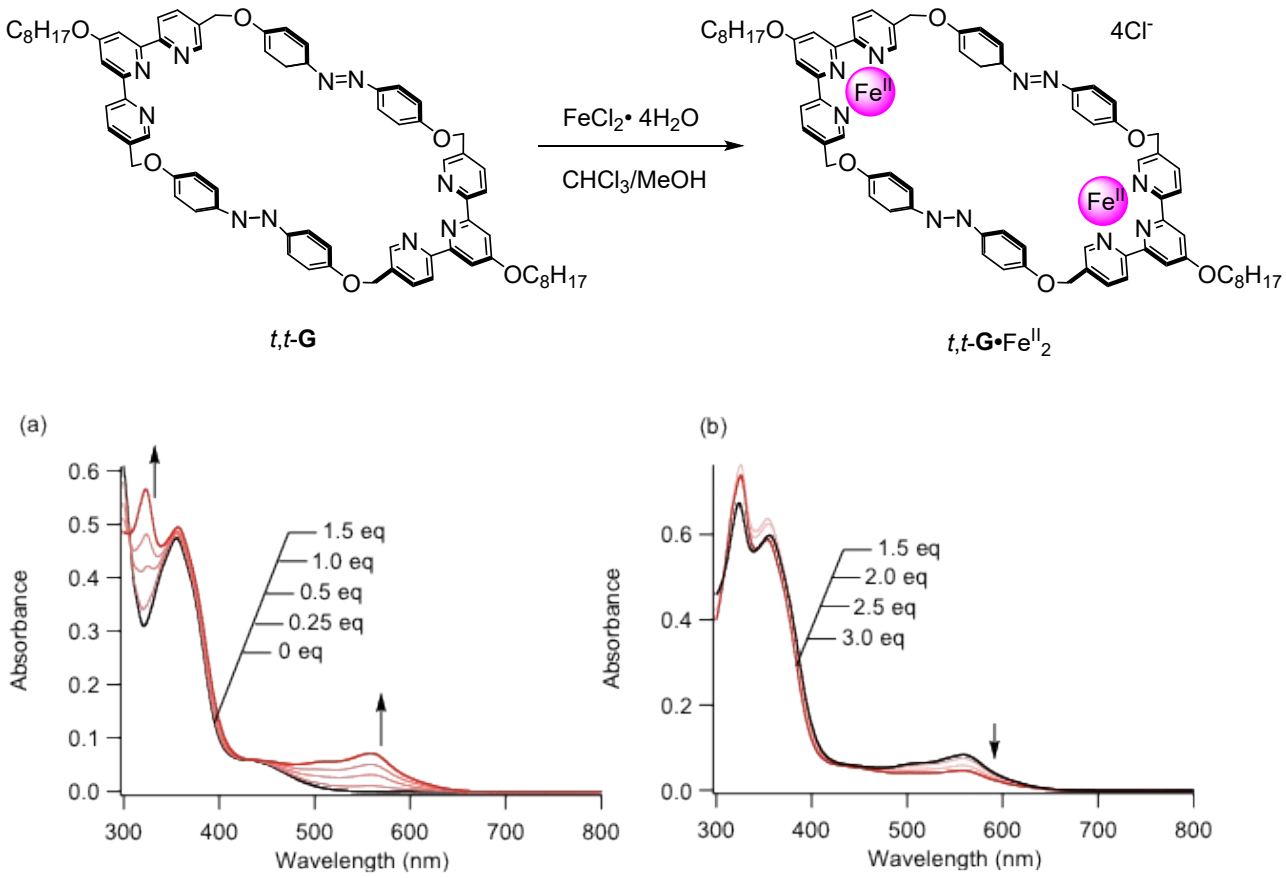

Figure S26. UV-Vis. spectral changes of *t*,*t*-**G** upon addition of $FeCl_2 \cdot 4H_2O$, $CHCl_3$/MeOH (1/1), 20 μM, l = 1 cm, a) $0 \leq [Fe^{II}]/[t,t\text{-}\mathbf{G}] \leq 1.5$, b) $1.5 \leq [Fe^{II}]/[t,t\text{-}\mathbf{G}] \leq 3.0$

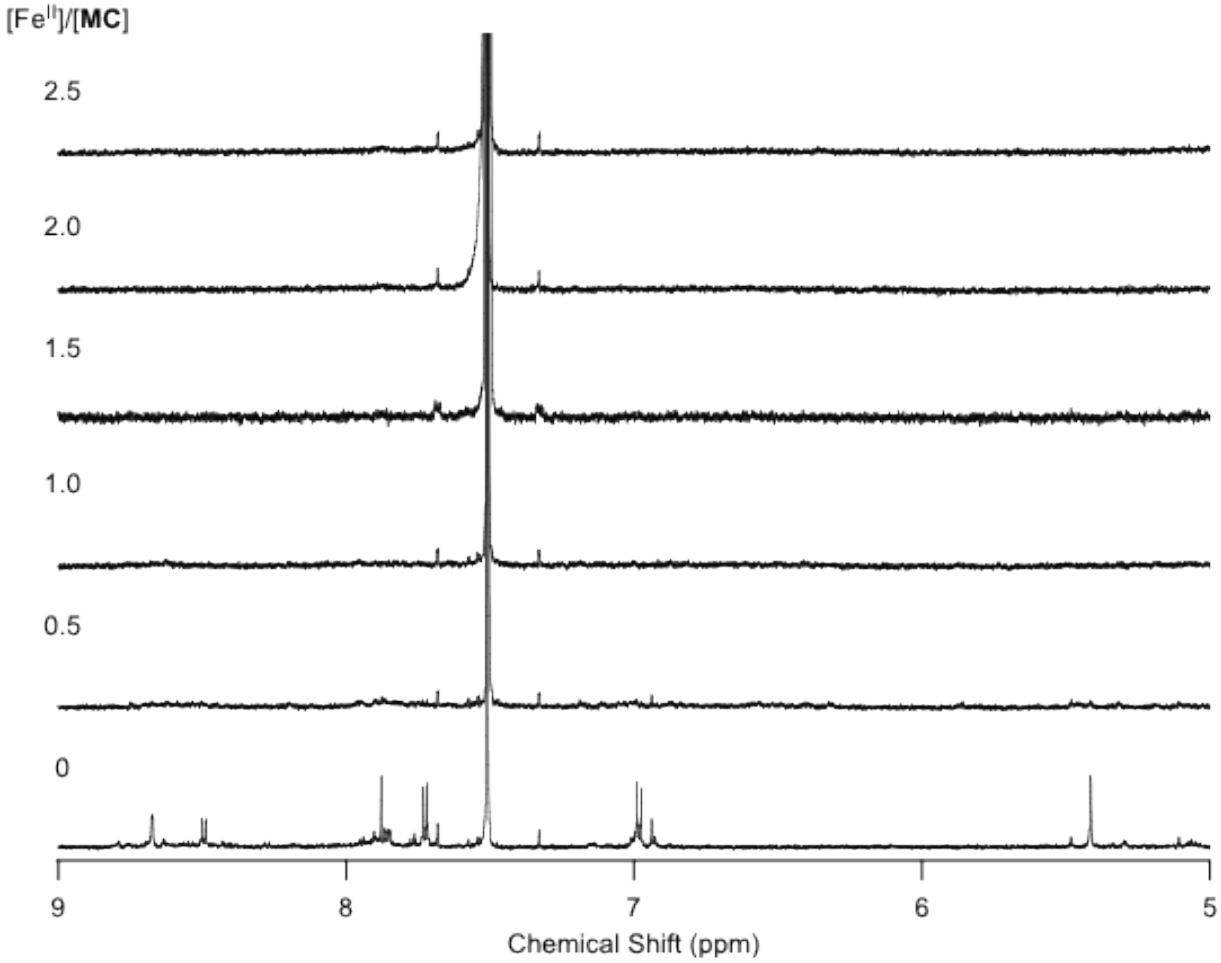

Figure S27. ^{1}H NMR spectral changes of *t*,*t*-**G** upon addition of addition of $FeCl_2 \cdot 4H_2O$, $CDCl_3/CD_3CN$ (3/2), [*t*,*t*-**G**] = 100 μM, 600 MHz

(7) Photoisomerization

Photoisomerization of *t*,*t*-**G**

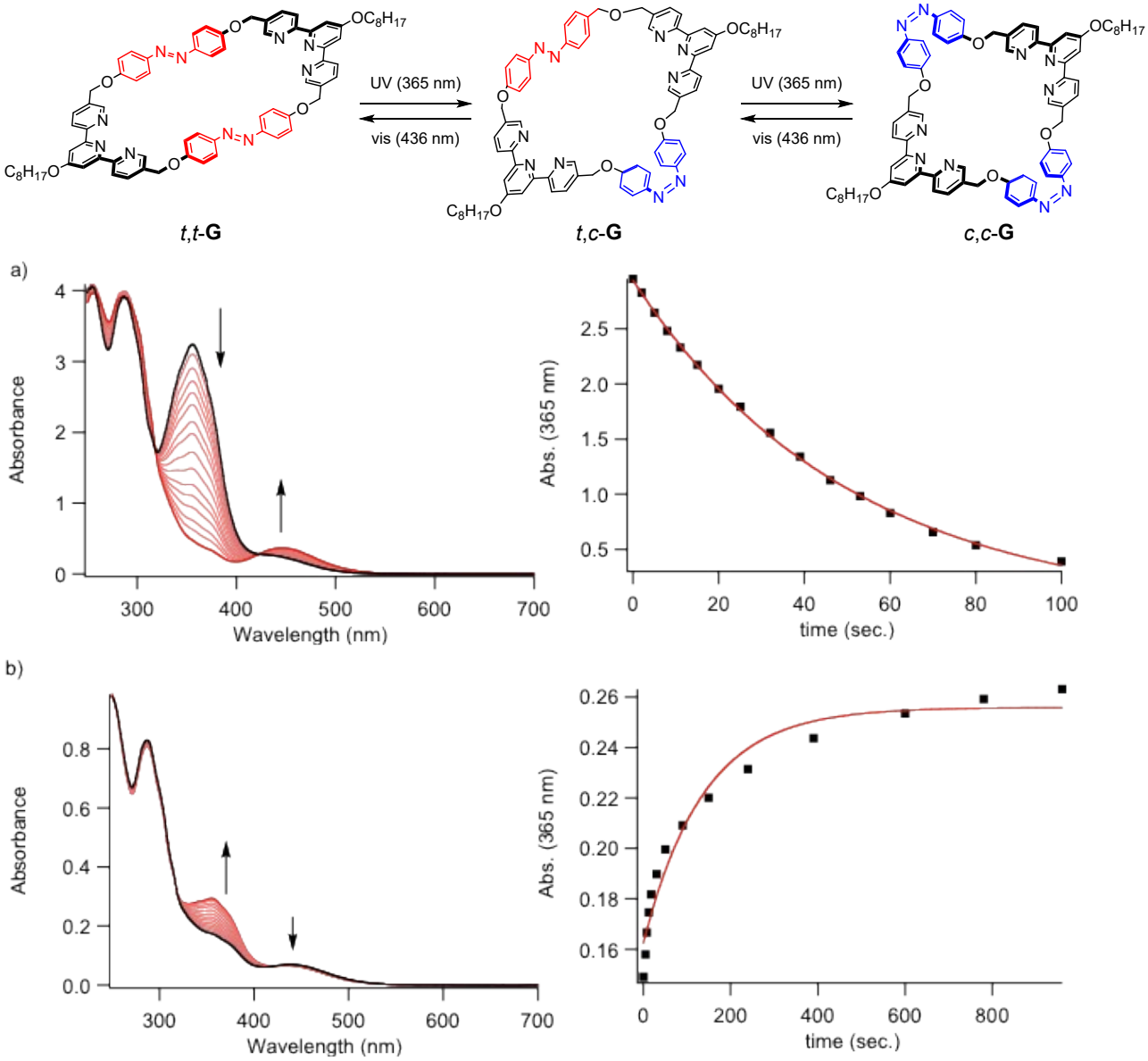

Figure S28. UV-vis spectral changes of *t*,*t*-**G** by irradiation of a) UV light (365 nm) for 0–420 sec. $CHCl_3$, 100 μM, l = 1 cm and b) visible light (436 nm) for 0–2700 sec. $CHCl_3$, 20 μM, l = 1 cm

The quantum yields of *trans*-to-*cis* isomerization were determined by kinetics for initial spectral changes according to the following equation. The photon flux (I_0) was determined by the measurement of the known isomerization of azobenzene itself.

$$\Phi_t = \frac{1}{I_0 \times \left(1 - 10^{A(t)}\right)} \frac{dA(t)}{\epsilon_t dt}$$

Φ_t: quantum yield of *trans*-to-*cis* isomerization, I_0: photon flux, $A(t)$: absorbance, ε_t: molar extinction coefficient

The quantum yields of *cis*-to-*trans* isomerization were determined by *cis*/*trans* ratio at the photostationary state.

$$\frac{\epsilon_t \times \Phi_t}{\epsilon_c \times \Phi_c} = \frac{[cis]_{pps}}{[trans]_{pps}}$$

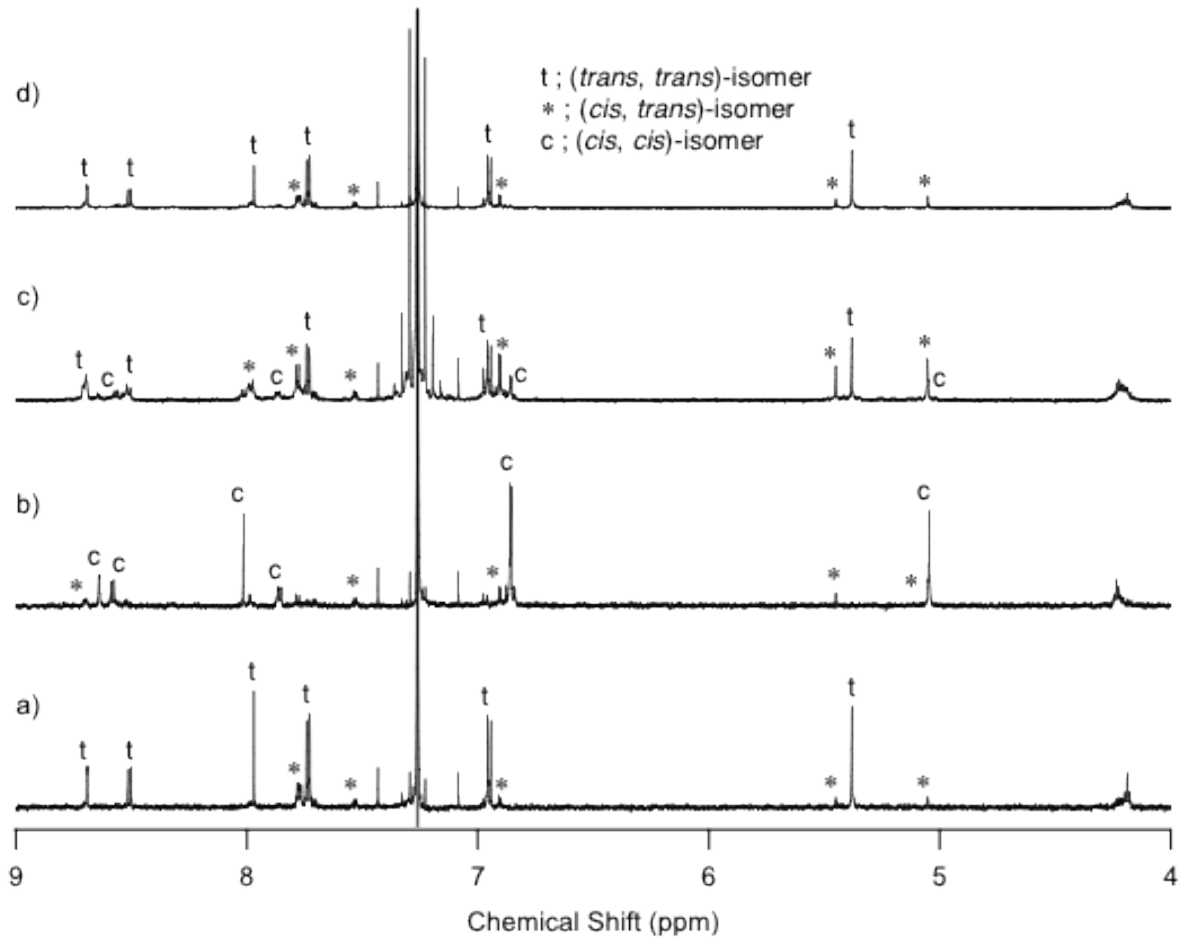

Figure S29. ^{1}H NMR spectra (400 MHz, $CDCl_3$) of *t*,*t*-**G** a) before and b) after photoirradiation of UV light (365 nm) c) after further photoirradiation of visible light (436 nm) d) after keeping in the dark at r.t. for 5 days.

Photoisomerization of [*t*,*t*-**G**·Zn^{II}_2·**L3**]$(ClO_4)_4$

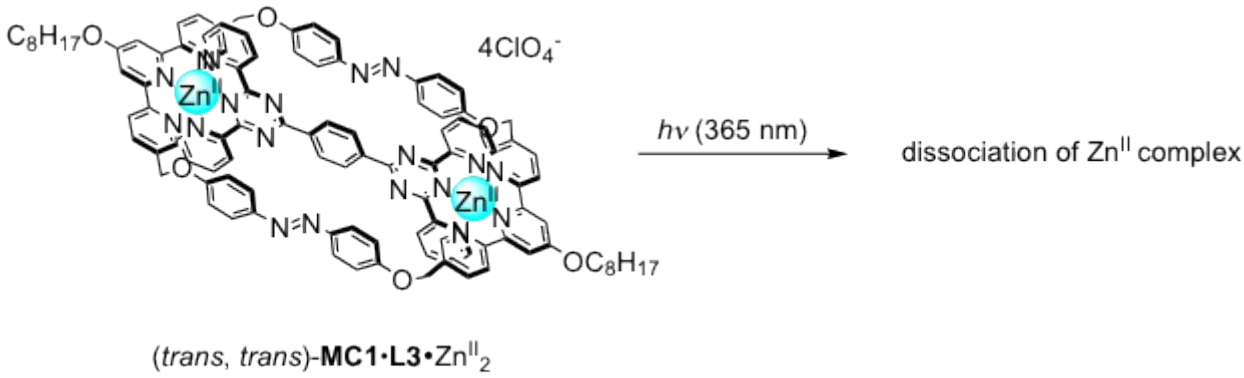

(*trans*, *trans*)-**MC1·L3•**Zn^{II}_2

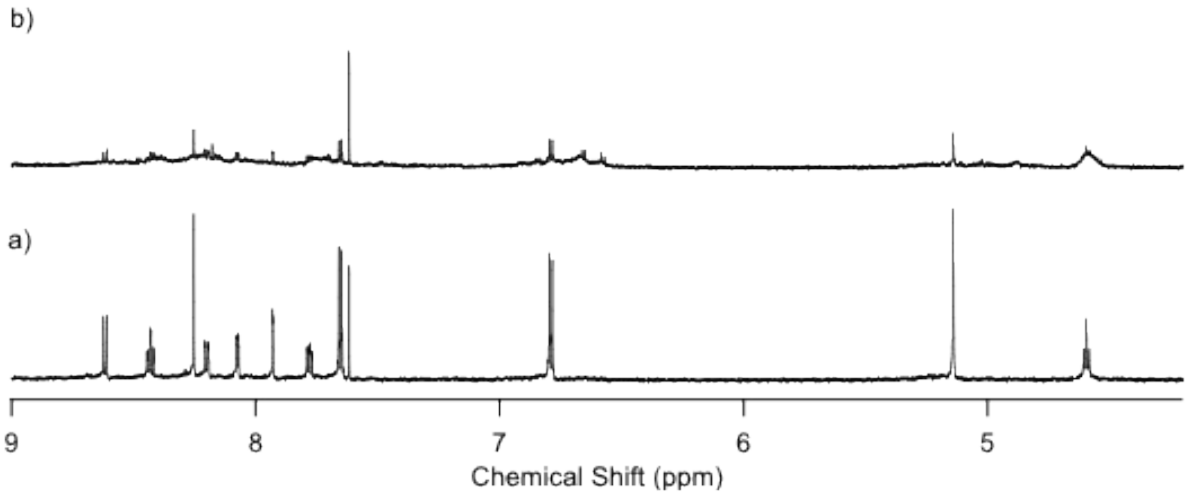

Figure S30. ^{1}H NMR spectrum (600 MHz, CD_3CN) of [*t*,*t*-**G**·Zn^{II}_2·**L3**]$(ClO_4)_4$ a) before and b) after photoirradiation of UV light (365 nm) for 30 min

Photoisomerization of [*t*,*t*-**G**·Fe^{II}_2·**L3**]$(PF_6)_4$

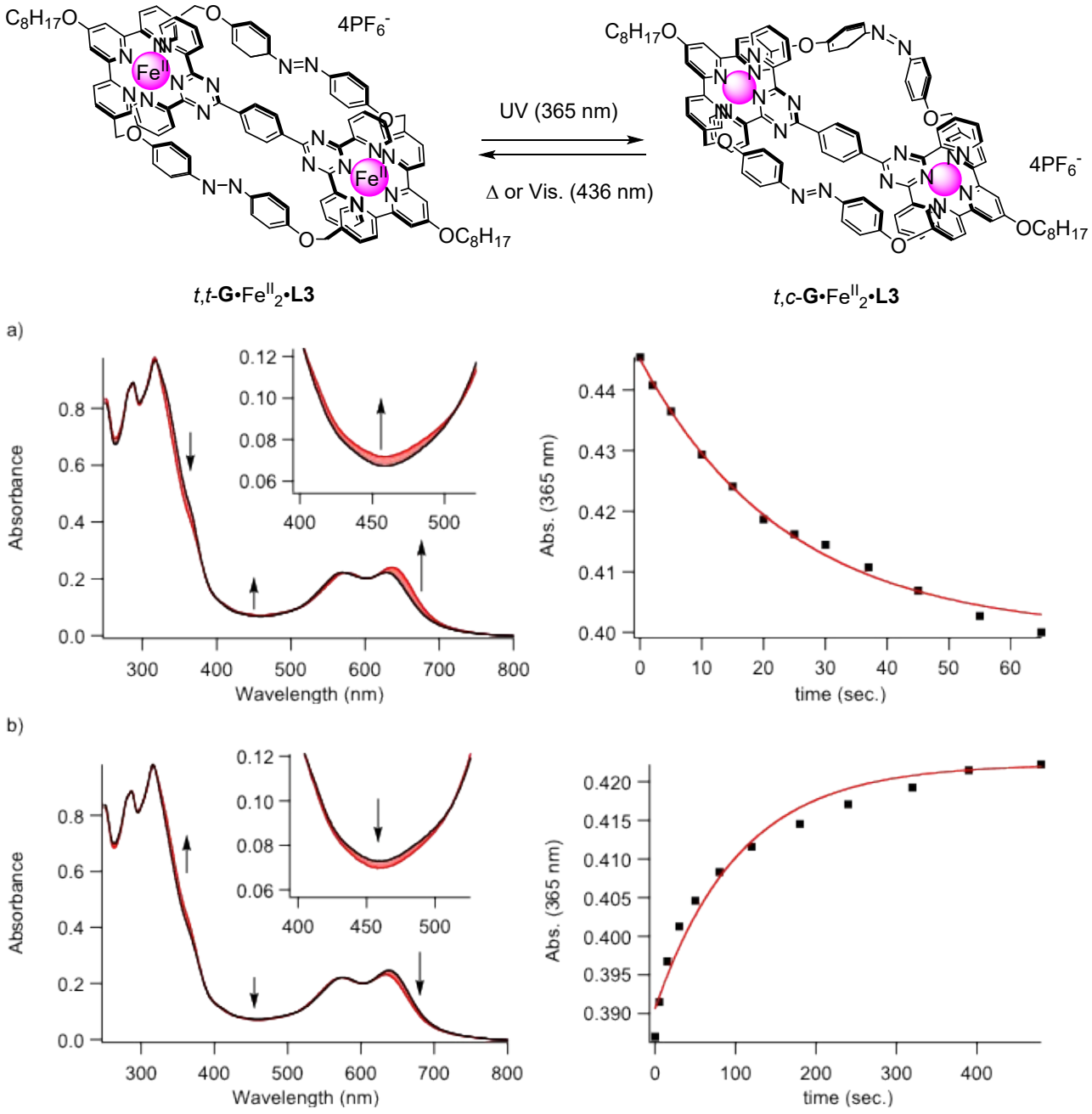

Figure S31. UV-Vis. spectral changes of [*t*,*t*-**G**·Fe^{II}_2·**L3**]$(PF_6)_4$ by irradiation of a) UV light (365 nm) for 0–60 sec. and b) visible light (436 nm) for 0–480 sec. CH_3CN, 10 μM, l = 1 cm.

Photoisomerization of [*t*,*t*-**G**·Fe^{II}_2·(**L4**)$_2$]$(PF_6)_4$

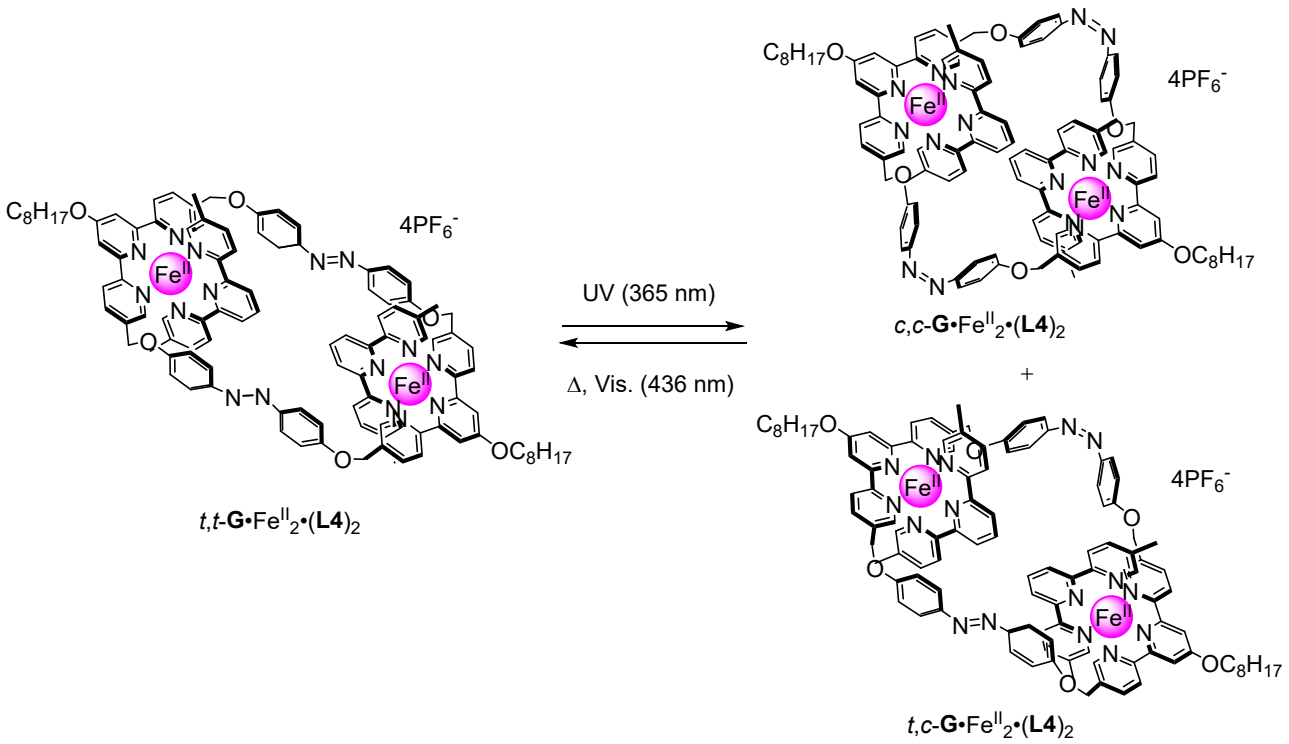

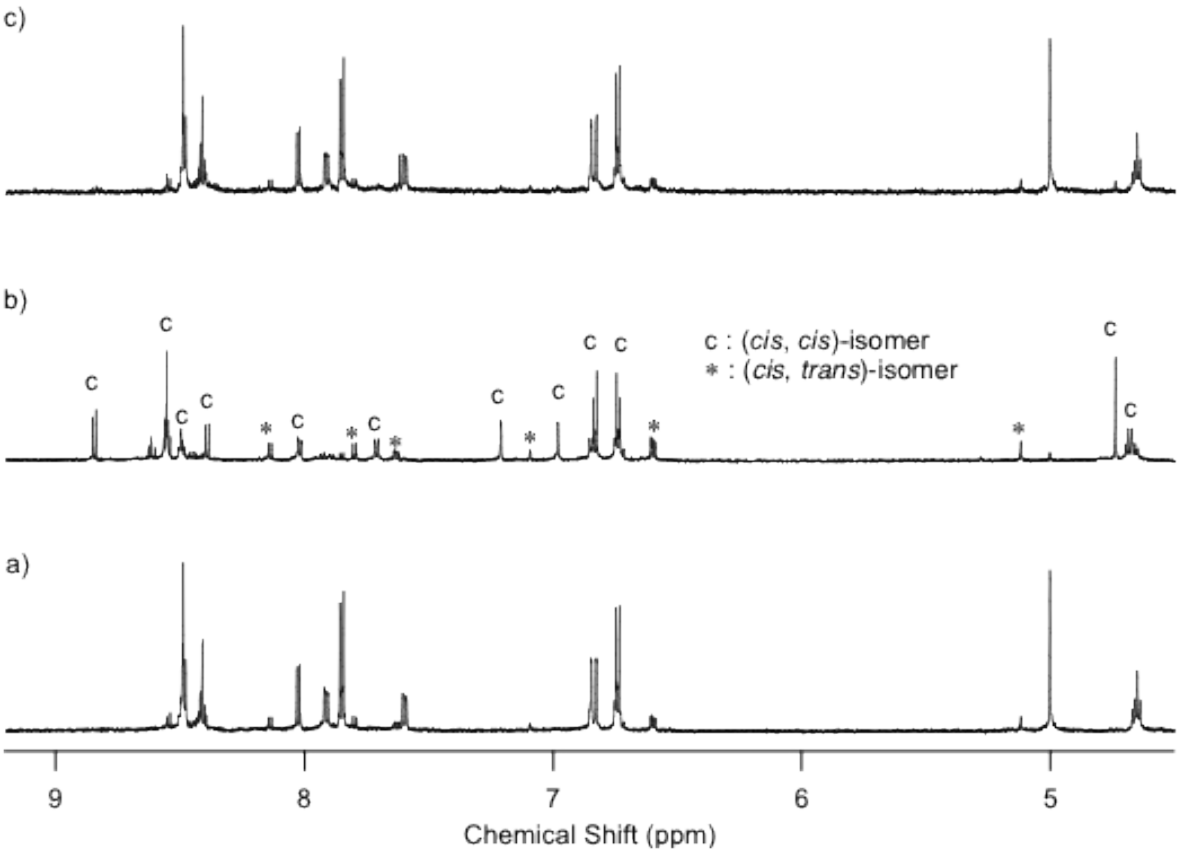

Figure S32. ^{1}H NMR spectra (600 MHz, $CDCl_3$) of [*t*,*t*-**G**·Fe^{II}_2·(**L4**)$_2$]$(PF_6)_4$ a) before and b) after photoirradiation of UV light (365 nm) for 45 min c) visible light (436 nm) for 90 min

Photoisomerization of [*c*,*c*-**G**·Fe^{II}]$(PF_6)_2$

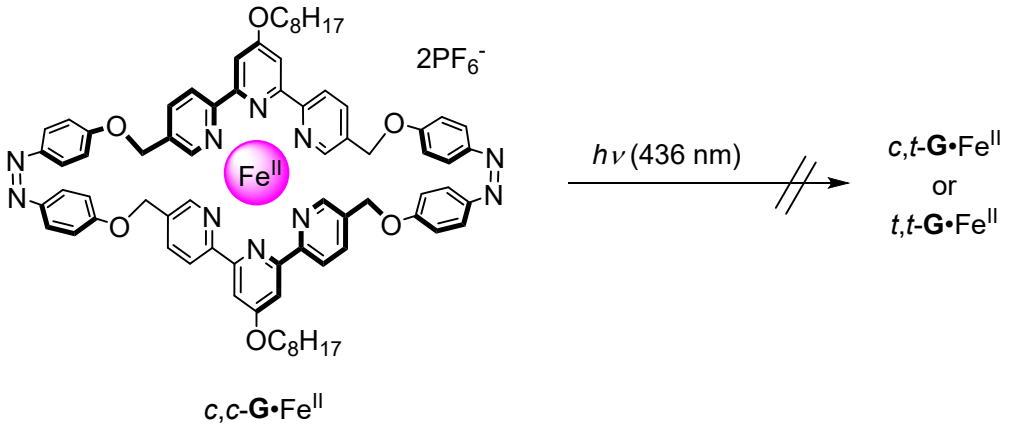

c,*c*-**G**•Fe^{II}

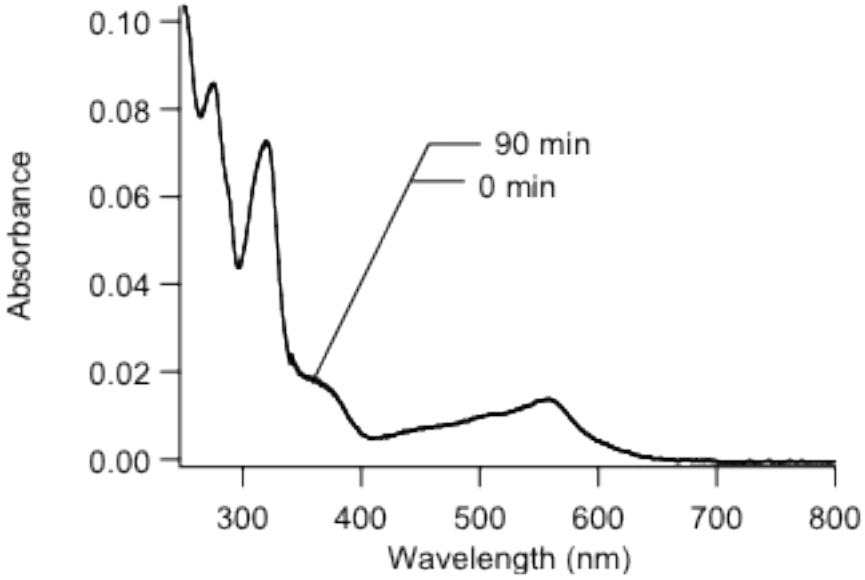

Figure S33. UV-Vis. spectral changes of [*c*,*c*-**G**·Fe^{II}]$(PF_6)_2$ by irradiation of visible light (436 nm) for 0, 90 min., CH_3CN, 1.0 μM, *l* = 1cm

(8) Thermal isomerization

Thermal isomerization of *c*,*c*-**G**

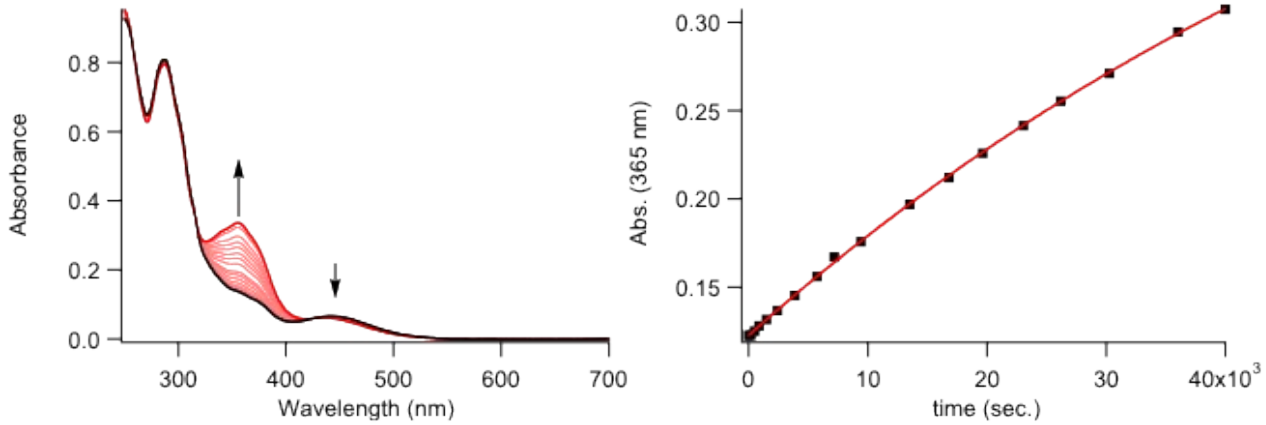

Figure S34. UV-Vis spectral changes of *c*,*c*-**G** heated at 30 ˚C, $CHCl_3$, 10 μM, *l* = 1 cm.

Thermal isomerization of [*c*,*t*-**G**·Fe^{II}_2·**L3**]$(PF_6)_4$

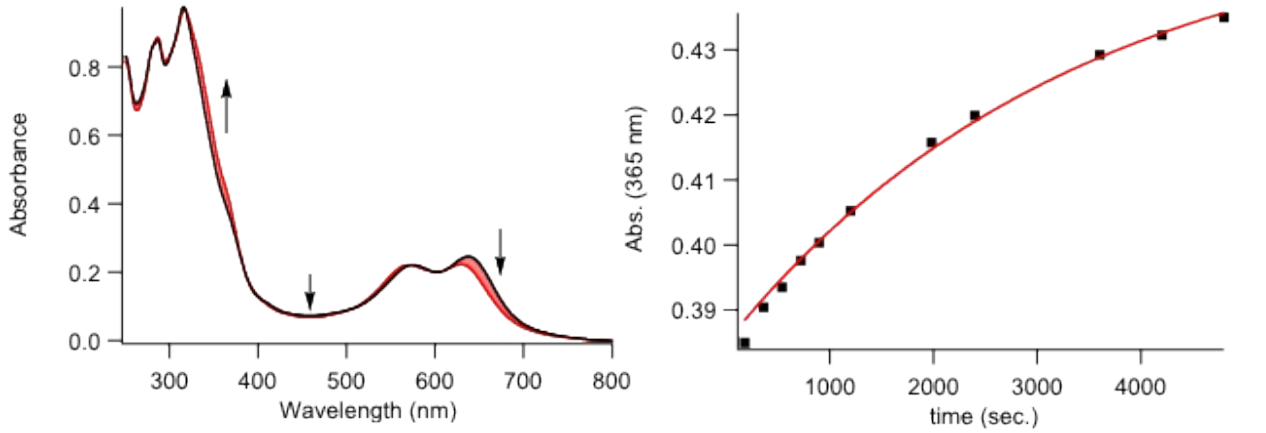

Figure S35. UV-Vis spectral changes of [*c*,*t*-**G**·Fe^{II}_2·**L3**]$(PF_6)_4$ heated at 30 ˚C, CH_3CN, 10 μM, *l* = 1 cm.

Thermal isomerization of [*c*,*c*-**G**·Fe^{II}]$(PF_6)_2$

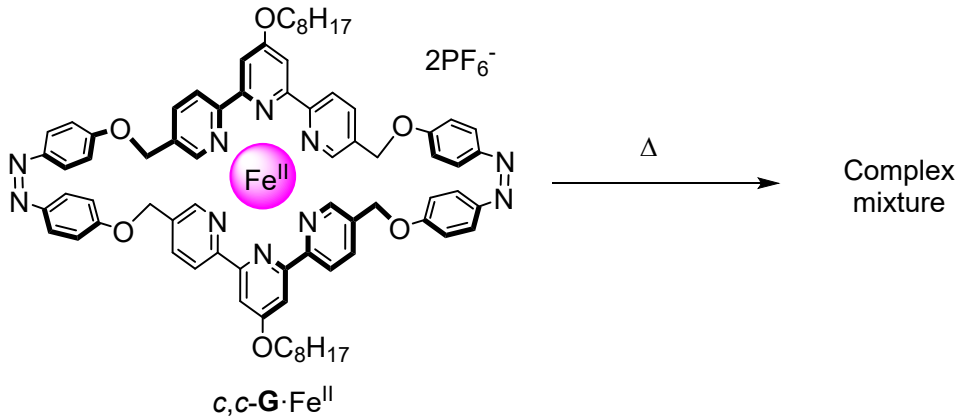

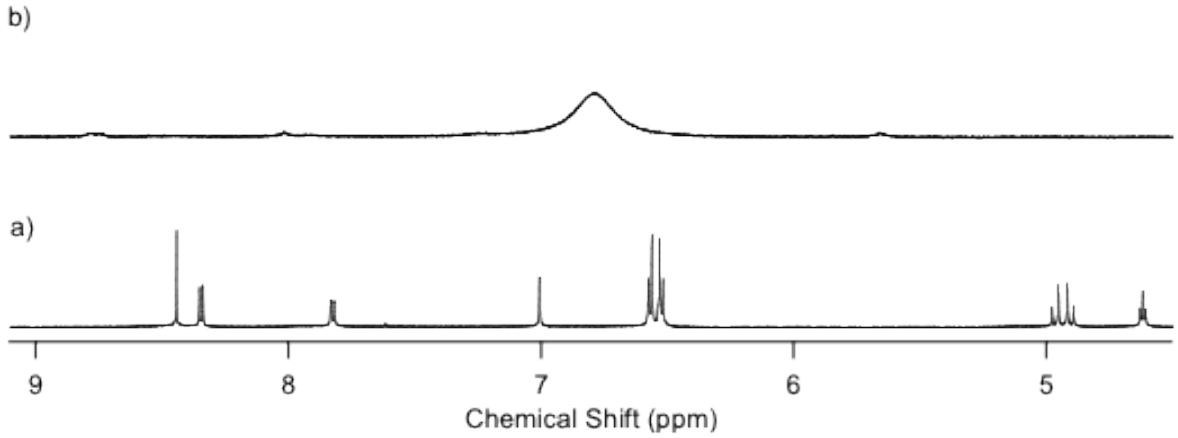

Figure S36. ^{1}H NMR spectra (600 MHz, CD_3CN) of [*c*,*c*-**G**·Fe^{II}]$(PF_6)_2$ a) before and b) after heated at 100 ˚C for 12 h

(9) Demetallation

To a 1.00 mL solution of [*c*,*c*-**G**·Fe^{II}]$(PF_6)_2$ in CH_3CN (100 μM) was added aqueous potassium hydroxide (0.5 M, 4 mL). A few drops of 30% H_2O_2 solution were then added slowly until the purple color diminished. The suspension was filtered through a millipore filter to remove iron oxides, and the filtrate was extracted with $CHCl_3$. This organic phase was dried over Na_2SO_4 and filtered. After evaporation of the solvent, the residual product was resolved into high-purified chloroform. The demetallation efficiency was determined to be 63% by UV-vis spectra based on the Lambert-Beer law. The demetallation efficiency of [*t*,*t*-**G**·Fe^{II}_2·**L3**]$(PF_6)_4$ was similarly determined to be 70%.

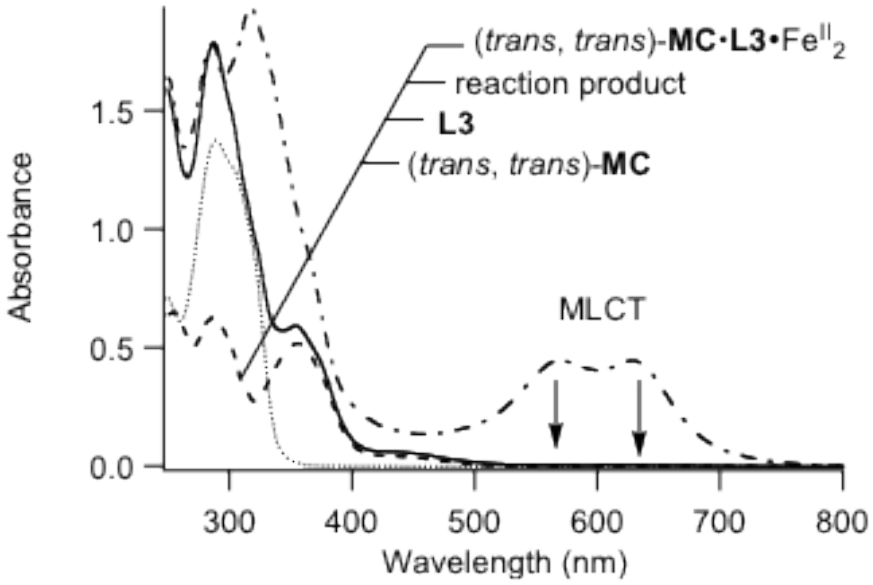

Figure S37. UV-vis spectral change of [*c*,*c*-**G**·Fe^{II}]$(PF_6)_2$ before (black, CH_3CN, 10 μM) and after treatment with H_2O_2 (red, $CHCl_3$).

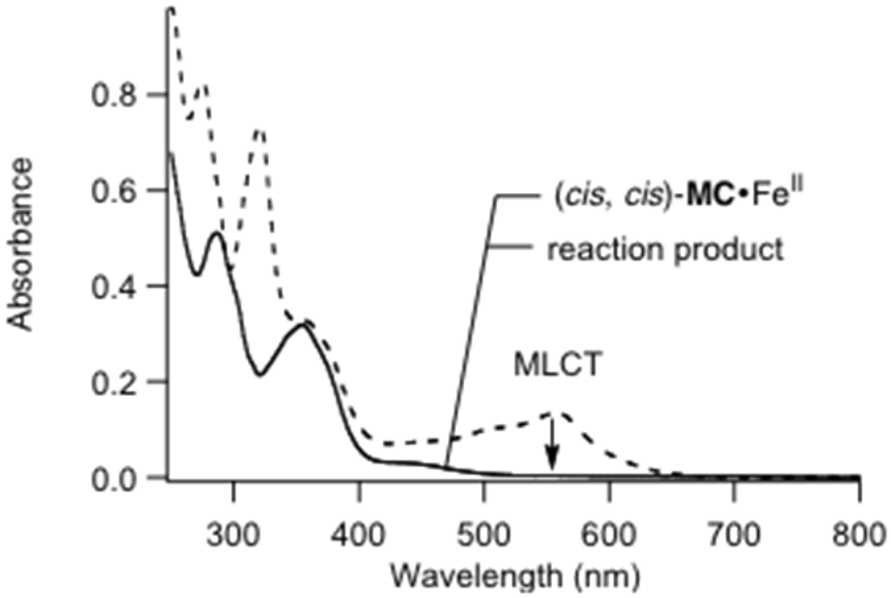

Figure S38. UV-vis spectral change of [*t*,*t*-**G**·Fe^{II}_2·**L3**]$(PF_6)_4$ before (black, CH_3CN, 10 μM) and after treatment with H_2O_2 (red, $CHCl_3$).

(10) Computational details

Equilibrium conformations of $[t,t\text{-}\mathbf{G}\cdot Fe^{II}_2\cdot\mathbf{L3}]^{4+}$, $[c,c\text{-}\mathbf{G}\cdot Fe^{II}]^{2+}$, and $[t,t\text{-}\mathbf{G}\cdot Fe^{II}_2\cdot(\mathbf{L4})_2]^{4+}$ were determined at the PM3 level using Spartan08 program.[S6] The geometry optimization of the equilibrium conformer was performed at the RM062X/6-31G(d,p) level using Gaussian09 program.[S7]

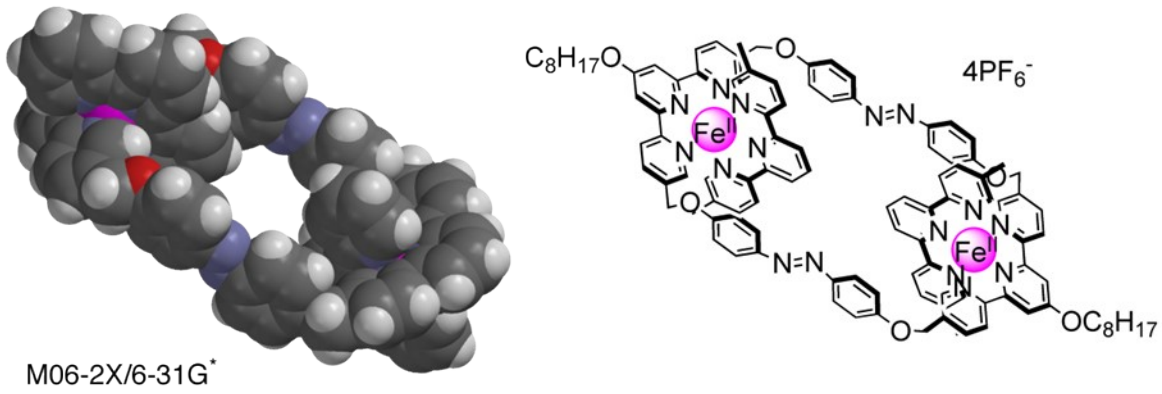

Figure S39. Equilibrium geometry of $[t,t\text{-}\mathbf{G}\cdot Fe^{II}_2\cdot(\mathbf{L4})_2]^{4+}$ at the RM062X/6-31G(d,p).

(11) References

S1 Abe, H.; Kurokawa, H.; Chida. Y.; Inouye, M. *J. Org. Chem.* **2011**, *76*, 309–311.

S2 Wei, W.-h.; Tomohiro, T.; Kodaka, M.; Okuno, H. *J. Org. Chem.* **2000**, *65*, 8979–8987.

S3 Glasson, C. R. K.; Meehan, G. V.; Motti, C. A.; Clegg, J. K.; Turner, P.; Jensen, P.; Lindoy, L. F. *Dalton Trans.* **2011**, *40*, 12153-12159.

S4 Grosshenny, V.; Harriman, A.; Gisselbrecht, J.-P.; Ziessel, R. *J. Am. Chem. Soc.* **1996**, *118*, 10315-10316.

S5 Santoni, M.-P.; Nastasi, F.; Campagna, S.; Hanan, G. S.; Hasenknopf, B.; Ciofini, I. *Dalton Trans.* **2013**, *42*, 5281-5291.

S6 Spartan 08, Wavefunction, Inc., **2008**.

S7 GAUSSIAN 09, Revision A.02, M. J. Frisch, G. W. Trucks, H. B. Schlegel, G. E. Scuseria, M. A. Robb, J. R. Cheeseman, G. Scalmani, V. Barone, B. Mennucci, G. A. Petersson, H. Nakatsuji, M. Caricato, X. Li, H. P. Hratchian, A. F. Izmaylov, J. Bloino, G. Zheng, J. L. Sonnenberg, M. Hada, M. Ehara, K. Toyota, R. Fukuda, J. Hasegawa, M. Ishida, T. Nakajima, Y. Honda, O. Kitao, H. Nakai, T. Vreven, J. A. Montgomery, Jr., J. E. Peralta, F. Ogliaro, M. Bearpark, J. J. Heyd, E. Brothers, K. N. Kudin, V. N. Staroverov, T. Keith, R. Kobayashi, J. Normand, K. Raghavachari, A. Rendell, J. C. Burant, S. S. Iyengar, J. Tomasi, M. Cossi, N. Rega, J. M. Millam, M. Klene, J. E. Knox, J. B. Cross, V. Bakken, C. Adamo, J. Jaramillo, R. Gomperts, R. E. Stratmann, O. Yazyev, A. J. Austin, R. Cammi, C. Pomelli, J. W. Ochterski, R. L. Martin, K. Morokuma, V. G. Zakrzewski, G. A. Voth, P. Salvador, J. J. Dannenberg, S. Dapprich, A. D. Daniels, Ö. Farkas, J. B. Foresman, J. V. Ortiz, J. Cioslowski, D. J. Fox, Gaussian, Inc., Wallingford CT, **2009**.